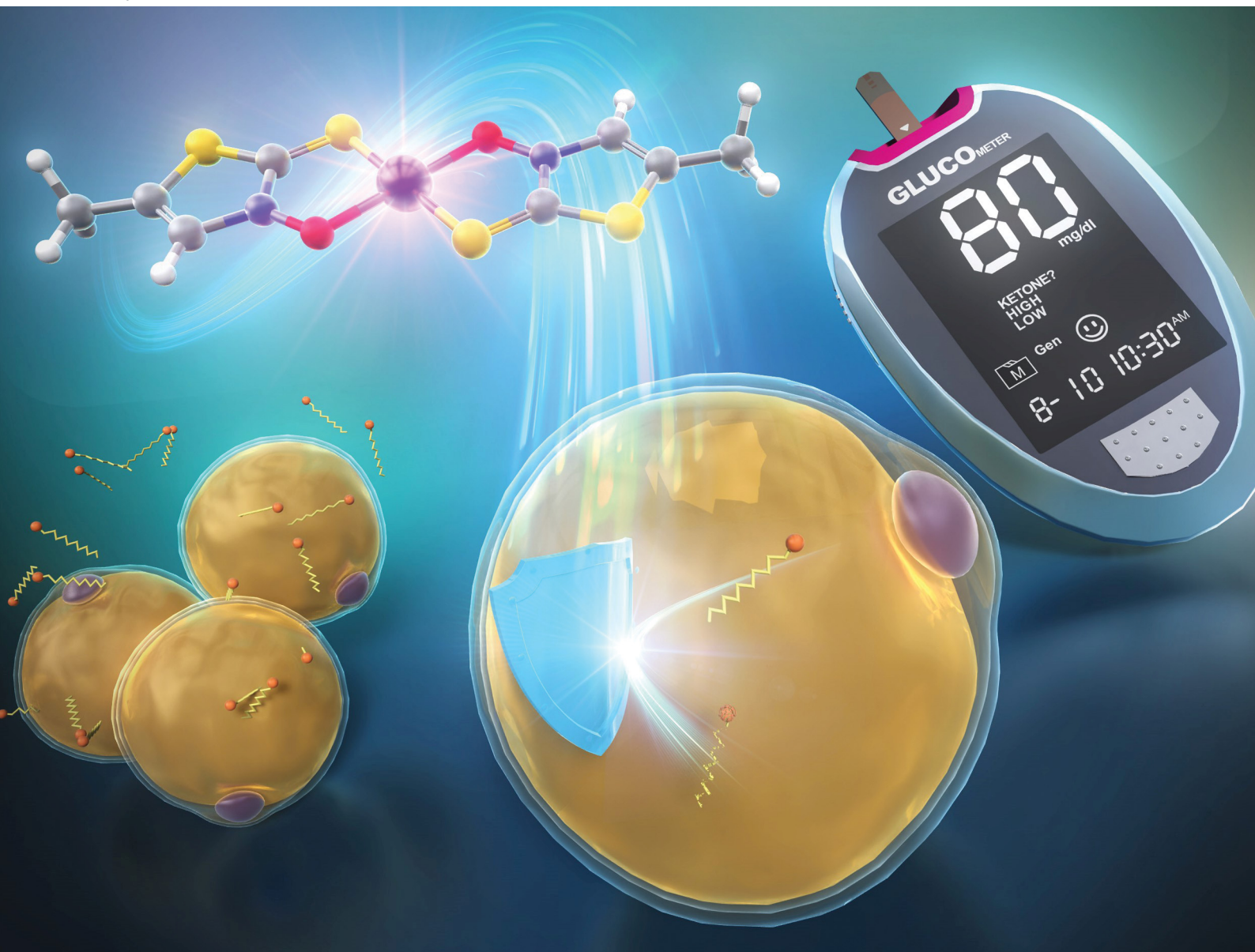


NJC

New Journal of Chemistry
rsc.li/njc

A journal for new directions in chemistry



ISSN 1144-0546

PAPER

Ryota Saito *et al.*

Synthesis, crystal structure, and insulin-mimetic activity of zinc(II) complexes with 4-alkyl- and 4,5-dialkyl-3-hydroxythiazole-2(3*H*)-thiones as a new class of hypoglycemic agent candidates


 Cite this: *New J. Chem.*, 2025, 49, 1145

Synthesis, crystal structure, and insulin-mimetic activity of zinc(II) complexes with 4-alkyl- and 4,5-dialkyl-3-hydroxythiazole-2(3H)-thiones as a new class of hypoglycemic agent candidates†

 Ryota Saito,^{ib}*^{ab} Yuki Naito,^{ib}^c Yutaka Yoshikawa,^d Hiroyuki Yasui,^c Shoko Kikkawa,^{ib}^e Huiyeong Ju,^f Rintaro Ohba,^a Tae Miyamoto,^a Shogo Sano,^a Kazuya Maeda,^a Mako Tamura^a and Isao Azumaya^{ib}^e

The development of potent hypoglycemic zinc complexes is important for treating diabetes mellitus. In this study, 3-hydroxythiazole-2(3H)-thiones (3,2-HTTs) with alkyl groups at the 4- and 4,5-positions were synthesized, and the insulin-mimetic activities of their zinc(II) complexes were evaluated by determining the 50% inhibitory concentration (IC₅₀) of free fatty acids released from isolated rat adipocytes treated with epinephrine. The structures of the complexes were unambiguously determined by means of X-ray crystallographic analyses. The IC₅₀ values of the newly synthesized complexes with 4,5-dialkyl-3,2-HTTs ranged from 16 to 24 μM, indicating higher inhibitory activities than those of previously reported 4-aryl-3,2-HTT-zinc(II) complexes (30–44 μM). The correlation between some properties of the complexes showed that complexes with smaller sizes tended to have higher insulin-mimetic activity. Besides, for all complexes, the stability constant were estimated to be less than 10.5, confirming the usefulness of the stability constant as a parameter for identifying zinc(II) complexes with high insulin-mimetic activity.

 Received 14th September 2024,
 Accepted 6th November 2024

DOI: 10.1039/d4nj04035j

rsc.li/njc

Introduction

Diabetes mellitus (DM) is a metabolic disease characterized by chronic hyperglycemia, which can result in various complications, such as nerve damage, retinopathy, kidney damage, atherosclerosis, and, in the worst case, death. The prevalence of diabetes is increasing annually, with projections indicating that by 2024, more than 12% of the global population aged 20–79

will be affected.¹ DM is generally classified into types 1 and 2.² In type 1 DM, there is an absolute shortage of insulin secretion owing to the destruction of insulin-secreting beta cells in the pancreas. Therefore, type 1 diabetics inevitably rely on insulin injections for their treatment. However, these injections impose significant financial and physical burdens. Type 2 DM, which accounts for >90% of diabetic patients,³ results from a deficiency in insulin action due to genetic predisposition and environmental and lifestyle factors, such as aging and obesity. The treatment of type 2 diabetes involves the administration of synthetic drugs, along with exercise and diet therapy. Currently, the most commonly used hypoglycemic agents include alpha-glucosidase inhibitors, which suppress the postprandial increase in blood glucose levels by degrading carbohydrates to delay their absorption; sulfonylureas, which stimulate insulin secretion; and thiazolidinediones, which improve insulin resistance by acting on insulin receptors.⁴ However, even with these drugs, blood glucose control is difficult and requires treatment with burdensome insulin injections.⁵ Therefore, it is imperative to develop a new drug that works *via* a different mechanism from conventional drugs and can be administered orally without burdensome insulin injections. Zinc ions have thus recently attracted considerable attention as novel drug candidates for DM. Zinc is an essential trace metal and is the second most

^a Department of Chemistry, Toho University, 2-2-1 Miyama, Funabashi, Chiba 274-8510, Japan. E-mail: saito@chem.sci.toho-u.ac.jp

^b Research Center for Materials with Integrated Properties, Toho University, 2-2-1 Miyama, Funabashi, Chiba 274-8510, Japan

^c Department of Analytical and Bioinorganic Chemistry, Kyoto Pharmaceutical University, Kyoto 607-8414, Japan

^d Department of Health, Sports and Nutrition, Kobe Women's University, 4-7-2 Minatojima-nakamachi, Chuo-ku, Kobe 650-0046, Japan

^e Faculty of Pharmaceutical Sciences, Toho University, 2-2-1 Miyama, Funabashi, Chiba, 274-8510, Japan

^f Western Seoul Center, Korea Basic Science Institute, 150 Bugahyeon-ro, Seodaemun-gu, Seoul 03759, South Korea

† Electronic supplementary information (ESI) available. CCDC 2379130 (for Zn(3)₂), 2383333 (for Zn(4)₂), 2383335 (for Zn(5f)₂), 2383331 (for Zn(5f)₂ + pyridine), 2383324 (for Zn(5h)₂), and 2383338 (for Zn(6)₂). For ESI and crystallographic data in CIF or other electronic format see DOI: <https://doi.org/10.1039/d4nj04035j>



abundant metal in the human body after iron.⁶ The optimal concentration range of zinc ions in the human body is wide and the risk of overdose poisoning is low.^{7–9} This makes the development of zinc ion-based drugs a highly attractive area of research. In 1980, Coulston and Dandona reported that zinc(II) ions stimulated lipogenesis in rat adipocytes in a manner similar to the action of insulin.¹⁰ Subsequently, it was found that oral administration of inorganic zinc salts, such as ZnCl₂ and ZnSO₄, could regulate glucose levels in blood plasma. However, the low bioavailability of inorganic zinc compounds, such as ZnCl₂ and ZnSO₄, necessitates higher doses, which can have adverse effects.¹¹ In response to this, based on the idea that an organic zinc(II) complex may increase the absorption rate of zinc ions, organic zinc(II) complexes were orally administered to rats and found to increase their bioavailability compared with inorganic ZnCl₂.^{11,12} This discovery led to the synthesis of several organozinc complexes to investigate their hypoglycemic effects and mechanisms of action. Sakurai *et al.* (2004) reported that a zinc(II) complex with picolinic acids as ligands exhibits insulin-mimetic activity by activating the insulin receptor and phosphatidylinositol 3-kinase. They also reported that zinc(II) complexes with maltol ligands exhibits insulin-mimetic activity by activating the glucose transporter GLUT4, which mediates insulin-stimulated glucose transport in adipocytes.¹³ In 2011, Yasui *et al.* demonstrated that a zinc(II) complex with 1-hydroxy-2(1H)-pyridinethione exhibited high insulin-mimetic activity because of the phosphorylation activation of Akt/PKB.¹⁴ According to Yoshikawa *et al.*, a zinc(II) complex with hinokitiol ligands promoted Akt/PKB phosphorylation, exhibiting high insulin-mimetic activity.¹⁵ These ligands were not designed specifically for zinc(II) complexes but are mainly known to complex with other metal ions, such as iron complexes. Hence, they are either commercially available, naturally occurring, or synthesized using established methods. To clarify the mechanism of action and develop more potent compounds, more detailed studies on the relationship between the structure of the ligands and the insulin-mimetic activity of their zinc(II) complexes are required. For this purpose, it is necessary to expand the compound library; therefore, the development of new synthetic ligands is imperative. Against this background, our research group focused on developing novel organic bidentate ligands for zinc(II)

complexes. Recently, we developed a new class of zinc(II) complexes with insulin-mimetic activity by demonstrating the insulin-mimetic activity of several zinc(II) complexes with 4-(*p*-substituted)phenyl-3-hydroxythiazole-2(3H)-thiones (**1**, Fig. 1) as ligands for the first time.¹⁶ Then, in the present study, which is part of our ongoing project involving the development of chemotherapeutics based on zinc(II) complexes of 3-hydroxythiazole-2(3H)-thione (3,2-HTT) derivatives, we synthesized several new zinc(II) complexes using 5-(*p*-substituted)phenyl-3,2-HTTs (**2** and **3**) and 4,5-dialkyl-3,2-HTTs (**4–6**) as ligands (Fig. 1). We also evaluated the *in vitro* insulin-mimetic activities of the new zinc(II) complexes and found that the new complexes with 4,5-dialkyl-3,2-HTTs exhibited increased insulin-mimetic activity.

Results and discussion

Zinc(II) complexes with the new ligand **2**, which are phenyl regioisomers of Zn(II) complexes with high insulin-mimetic activity, were prepared according to Scheme 1. First, aldehydes **7a**, **7f**, and **7g** were reacted with hydroxylamine hydrochloride to obtain the corresponding oximes **8a**, **8f**, and **8g**, respectively. The oxime hydroxyl group was protected by TBSCl. AIBN-initiated radical bromination reactions of TBS-protected

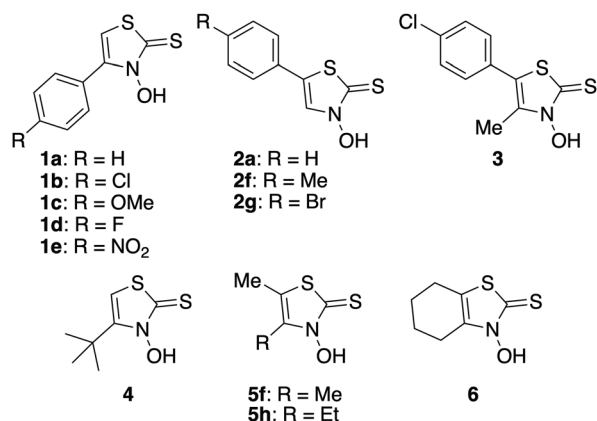
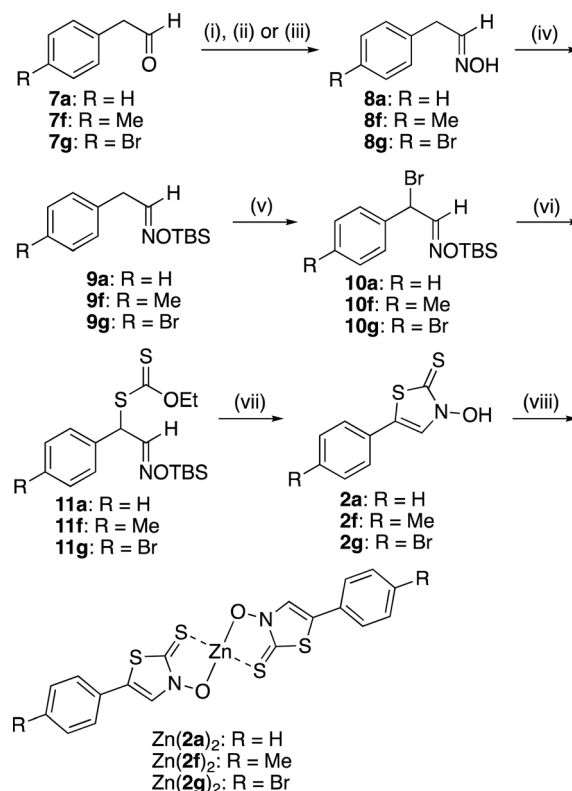


Fig. 1 Structures of 3-hydroxythiazole-2(3H)-thione (3,2-HTT) derivatives.



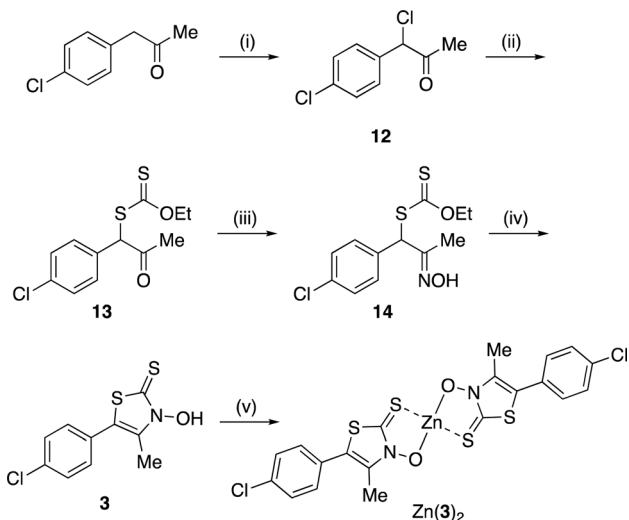
Scheme 1 Reagents and conditions: (i) NH₂OH·HCl, Na₂CO₃, 50% methanol aq., room temperature (r.t.), 2.5 h (for **7a**); (ii) NH₂OH·HCl, pyridine, ethanol, 85 °C, 4 h (for **7f**); (iii) NH₂OH·HCl, pyridine, methanol, r.t., 4 h (for **7g**); (iv) TBSCl, imidazole, CH₂Cl₂, 0 °C to r.t., 3–4 h; (v) NBS, AIBN, CCl₄, reflux, 3 h; (vi) potassium *O*-ethyl dithiocarbonate, acetone, r.t., 16–26 h; (vii) ZnCl₂, Et₂O, 0 °C to r.t., 6–8 d, then HCl aq.; (viii) Zn(OAc)₂, LiOH, H₂O/EtOH, r.t., 1–3 h.



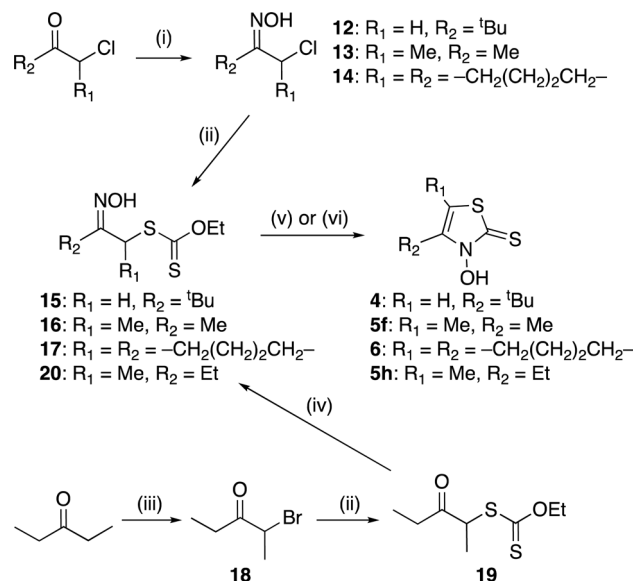
oximes **9a**, **9f**, and **9g** yielded the corresponding bromides **10a**, **10f**, and **10g**, respectively. The bromides were then reacted with potassium *O*-ethyl dithiocarbonate to obtain the corresponding xanthates (**11a**, **11f**, and **11g**). Intramolecular cyclocondensation of **11a**, **11f**, and **11g** was achieved using potassium hydroxide to form new ligands **2a**, **2f**, and **2g**, respectively. The zinc(II) complexes **2a**, **2f**, and **2g** were furnished by reacting **11a**, **11f**, and **11g**, respectively, with zinc acetate in the presence of lithium hydroxide.

A zinc(II) complex of **3** ($\text{Zn}(\mathbf{3})_2$) was obtained, as shown in Scheme 2. α -Chlorination of (*p*-chlorophenyl)acetone with suluryl chloride,¹⁷ followed by nucleophilic substitution with potassium *O*-ethyl dithiocarbonate, yielded xanthate **13**, which was converted into the corresponding oxime **14** with hydroxylamine hydrochloride.¹⁷ The same cyclocondensation reaction used in the synthesis of **2** yielded the targeted 3,2-HTT **3**.¹⁷ Subsequently, **3** was reacted with zinc perchlorate, yielding $\text{Zn}(\mathbf{3})_2$. Notably, $\text{Zn}(\mathbf{3})_2$ was obtained in high yield, even in the absence of lithium hydroxide.

Ligands **4**, **5f**, **5h**, and **6** were synthesized from the appropriate α -chloroketones, which were converted into the corresponding oximes **12–14** using hydroxylamine hydrochloride (Scheme 3). In contrast to the reactions in Schemes 1 and 2, these reactions require low-temperature conditions.¹⁸ When these oxidation reactions were performed under the same conditions as those in Schemes 1 and 2, multiple unisolable products were formed, and the desired chloride was not detected. Oximes **12–14** were then reacted with *O*-ethyl dithiocarbonate to obtain xanthates **15–17**. Meanwhile, 2-bromo-3-pentanone (**18**), which was prepared from 3-pentanone and bromine,^{19,20} was treated with *O*-ethyl dithiocarbonate to obtain xanthate **19**.^{17,21} Subsequently, **19** was converted into the corresponding oxime **20**. In this case, the reaction conditions used for



Scheme 2 Synthetic route to zinc(II) $\text{Zn}(\mathbf{3})_2$. Reagents and conditions: (i) SO_2Cl_2 , CH_2Cl_2 , 0 °C to r.t., 22 h, quant.; (ii) potassium *O*-ethyl dithiocarbonate, acetone, r.t., 4 h, quant.; (iii) $\text{NH}_2\text{OH}\cdot\text{HCl}$, aqueous ethanol, r.t., 21 h, 91%; (iv) KOH , aqueous CH_2Cl_2 , r.t., 48 h, 29%; (v) $\text{Zn}(\text{ClO}_4)_2\cdot 6\text{H}_2\text{O}$, aqueous ethanol, r.t., 1 h, 75%.



Scheme 3 Synthetic route to zinc(II) $\text{Zn}(\mathbf{4})_2$, $\text{Zn}(\mathbf{5f})_2$, $\text{Zn}(\mathbf{5h})_2$, and $\text{Zn}(\mathbf{6})_2$. Reagents and conditions: (i) $\text{NH}_2\text{OH}\cdot\text{HCl}$, CH_3COONa , water, -20 °C, 19–20 h; (ii) potassium *O*-ethyl dithiocarbonate, acetone, r.t., 2.5–19.5 h; (iii) Br_2 , Et_2O , r.t., 45 min; (iv) $\text{NH}_2\text{OH}\cdot\text{HCl}$, pyridine, methanol, r.t., 11 h; (v) ZnCl_2 , Et_2O , 0 °C to r.t., 43–66 h, then HCl aq. (for **15–17**); (vi) KOH , CH_2Cl_2 , 0 °C to r.t., 2.5 h, then HCl aq. (for **20**); (vii) $\text{Zn}(\text{OAc})_2\cdot 2\text{H}_2\text{O}$, $\text{H}_2\text{O}/\text{EtOH}$, r.t., 2–2.5 h.

the preparation of **8g** were employed. The obtained xanthates (**15–17** and **20**) were subjected to cyclocondensation reactions, yielding the targeted 3,2-HTTs **4–6** (Scheme 3).

The synthesized 3,2-HTTs (**4**, **5f**, **5h**, and **6**) were reacted with half the equimolar amount of zinc acetate dihydrate to form the desired zinc(II) complexes in high yield (Fig. 2). Structural determination of these complexes was performed *via* ^1H - and ^{13}C -NMR, infrared (IR) spectroscopy, and combustion analysis. Upon complexation with zinc(II) ions, the OH signals of the ligands in ^1H -NMR disappeared (Fig. 3), and all the carbon signals of the $\text{C}=\text{S}$ groups shifted upfield (Fig. 4). In the IR

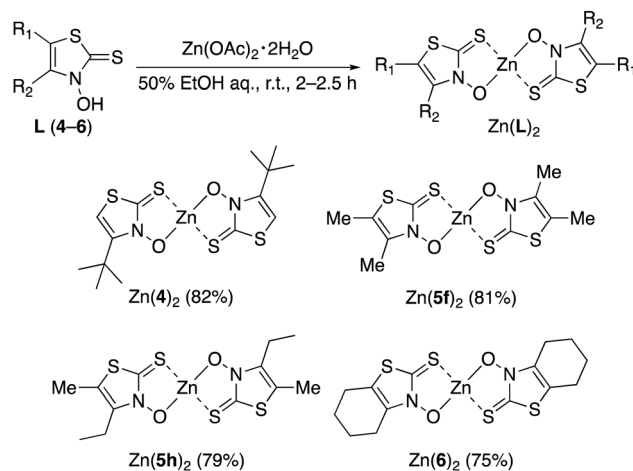


Fig. 2 Complexation reactions for the synthesis of zinc(II) complexes having 3,2-HTT ligands.

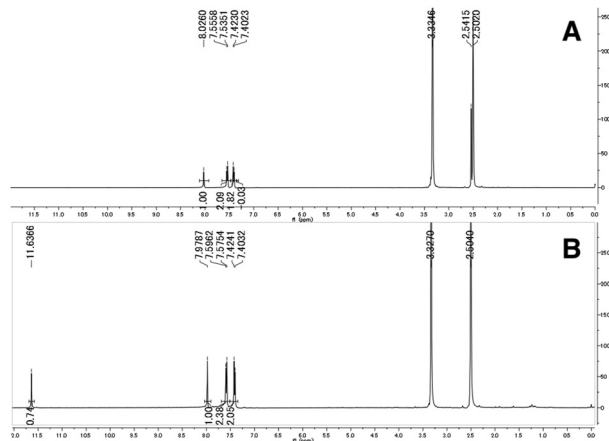


Fig. 3 Selected ^1H -NMR spectra of **2f** (A) and $\text{Zn}(\mathbf{2f})_2$ (B) in dimethyl sulfoxide- d_6 .

spectra, for all the ligands, the peaks corresponding to the C=S stretching vibrations, which are generally observed at approximately 1600 cm^{-1} , of the thiocarbonyl groups were shifted to lower wavenumbers upon complexation (see Experimental section). Similar spectral changes were observed upon complexation of **1a–e** with zinc(II) ions.¹⁶

The zinc-ligand stoichiometry and binding modes of all the complexes were unambiguously determined *via* X-ray crystallographic analysis. The zinc(II) complexes $\text{Zn}(\mathbf{4})_2$, $\text{Zn}(\mathbf{5f})_2$, $\text{Zn}(\mathbf{5h})_2$, and $\text{Zn}(\mathbf{6})_2$ were soluble in organic solvents, and single crystals suitable for X-ray diffraction analysis were obtained from a dichloromethane/*n*-hexane binary solvent system.²² The crystallographic data are summarized in Table 1. The crystals of $\text{Zn}(\mathbf{4})_2$, $\text{Zn}(\mathbf{5f})_2$, and $\text{Zn}(\mathbf{6})_2$ were monoclinic, with space groups $P2_1/n$, $P2_1/c$, and $C2/c$, respectively. $\text{Zn}(\mathbf{5h})_2$ crystallized in the triclinic space group $P\bar{1}$ (Table 1). Their solid-state structures are shown in Fig. 5, proving that the 4,5-dialkyl-3,2-HTT ligands coordinate to zinc(II) ions with a 1 : 2 metal-to-ligand ratio and in the *trans* S_2O_2 mode. In all cases, the coordination geometries around the central zinc(II) ions were tetrahedral. Selected

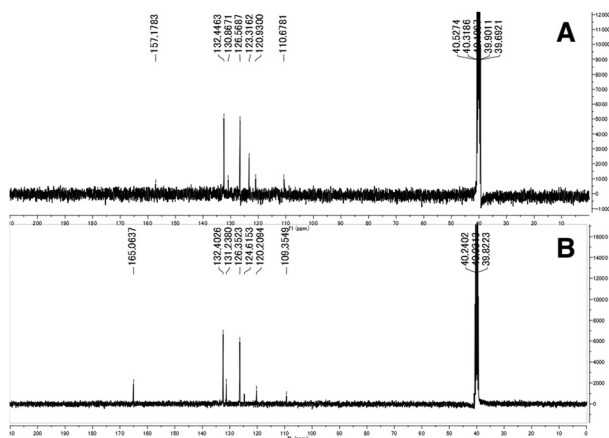


Fig. 4 Selected ^{13}C -NMR spectra of **2f** (A) and $\text{Zn}(\mathbf{2f})_2$ (B) in dimethyl sulfoxide- d_6 .

bond distances and angles are presented in Table 2. The bond angles reveal that one of the two siemens–Zn–O angles is nearly 90° for all the complexes, whereas the other S–Zn–O, S–Zn–S, and O–Zn–O angles exhibit considerable variation (109.87° to 129.29°). The central angle of a tetrahedron is approximately 109.5° . Therefore, the tetrahedral coordination of these zinc(II) complexes was highly distorted. In contrast, $\text{Zn}(\mathbf{2a})_2$, $\text{Zn}(\mathbf{2f})_2$, $\text{Zn}(\mathbf{2g})_2$, and $\text{Zn}(\mathbf{3})_2$, which are composed of ligands containing phenyl rings, are poorly soluble in conventional organic solvents, and attempts to obtain single crystals for X-ray crystallographic analysis were unsuccessful in all but one case. The only exception was $\text{Zn}(\mathbf{3})_2$, for which single crystals were obtained from dimethyl formamide with pyridine as an auxiliary solvent. The solved crystal data details for $\text{Zn}(\mathbf{3})_2$ are compiled in Table 1, and the molecular structure of $\text{Zn}(\mathbf{3})_2$ is depicted in Fig. 6(A).

$\text{Zn}(\mathbf{3})_2$ crystallizes in the monoclinic space group $P2_1/c$. As shown in Fig. 6(A), $\text{Zn}(\mathbf{3})_2$ has a square pyramidal structure with a 1 : 2 metal-to-ligand ratio and a *trans* S_2O_2 mode. In this case, a pyridine molecule is bound to the central zinc(II) ion at the apical position. Similar examples of solvent molecules coordinating to zinc(II) ions from apical positions have been observed in $\text{Zn}(\mathbf{1b})_2$ and $\text{Zn}(\mathbf{1d})_2$.¹⁶ These results suggest that the 3,2-HTTs/Zn complexes have one coordinating solvent molecule apically when a coordinating solvent is present in the medium. To confirm this, we recrystallized $\text{Zn}(\mathbf{5f})_2$ from a pyridine/*n*-hexane binary solvent system and subjected the resulting single crystals to X-ray crystallographic analysis. As a result, apical coordination of pyridine to the central zinc atom was observed (Fig. 6(B)). From these results, it can be concluded that water molecules coordinate apically *in vivo* and assume a square pyramidal state, as observed in a zinc(II) complex with 4-methyl-3,2-HTT ligands reported by Bond *et al.*²³

The insulin-mimetic activities of the synthesized zinc(II) complexes $\text{Zn}(\mathbf{2a})_2$ – $\text{Zn}(\mathbf{6})_2$ *in vitro* were evaluated by measuring the effects of the complexes on free fatty acid (FFA) release from rat adipose cells stimulated with epinephrine. This is a simple and reliable method for assessing the insulin-mimetic activity of materials.^{24–27} The results are shown in Fig. 7. Of the nine complexes tested, six exhibited inhibitory activity toward the FFA release in a dose-dependent manner: $\text{Zn}(\mathbf{2a})_2$, $\text{Zn}(\mathbf{2g})_2$, $\text{Zn}(\mathbf{4})_2$, $\text{Zn}(\mathbf{5f})_2$, $\text{Zn}(\mathbf{5h})_2$, and $\text{Zn}(\mathbf{6})_2$. This indicated that these complexes had insulin-mimetic activity. No significant inhibitory effects were observed for $\text{Zn}(\mathbf{2f})_2$ or $\text{Zn}(\mathbf{3})_2$. According to these results, the inhibitory activities of the six complexes were quantified by calculating the IC_{50} value, which represents the concentration of a complex at which FFA release from isolated rat adipocytes was inhibited by 50%. The results are summarized in Table 3. The insulin-mimetic activities (*i.e.*, IC_{50} values) of the complexes having mono- and di-alkyl-3,2-HTT ligands (**4–6**) ranged from 16–24 μM , all of which were higher than those of $\text{Zn}(\mathbf{2a})_2$ and $\text{Zn}(\mathbf{2f})_2$, which have phenyl groups at the C5 position of the 3,2-HTT skeleton. These results indicate that the introduction of a more hydrophobic phenyl group reduced the insulin-mimetic activity of zinc(II) complexes with 3,2-HTT ligands. However, it has been reported that zinc complexes with **1a–e**, which have phenyl groups, exhibit high insulin-mimetic



Table 1 Selected crystallographic data for Zn(3)₂, Zn(4)₂, Zn(5f)₂, Zn(5h)₂ and Zn(6)₂

Complex	Zn(4) ₂	Zn(5f) ₂	Zn(5h) ₂	Zn(6) ₂	Zn(3) ₂ (with pyridine)	Zn(5f) ₂ (with pyridine)
Formula	C ₁₀ H ₁₂ N ₂ O ₂ S ₆ Zn	C ₁₀ H ₁₂ N ₂ O ₂ S ₄ Zn	C ₁₂ H ₁₆ N ₂ O ₂ S ₄ Zn	C ₁₄ H ₁₆ N ₂ O ₂ S ₄ Zn	C ₂₅ H ₁₉ Cl ₂ N ₃ O ₂ S ₄ Zn	C ₁₅ H ₁₇ N ₃ O ₂ S ₄ Zn
<i>F</i> _w	441.93	385.83	413.88	437.90	657.97	464.93
Crystal system	Monoclinic	Monoclinic	Triclinic	Monoclinic	Monoclinic	Monoclinic
Space group	<i>P</i> 2 ₁ / <i>n</i>	<i>P</i> 2 ₁ / <i>c</i>	<i>P</i> $\bar{1}$	<i>C</i> 2/ <i>c</i>	<i>P</i> 2 ₁ / <i>c</i>	<i>P</i> 2 ₁
Temperature(K)	120	120	120	120	93	120
<i>a</i> /Å	8.6523(3)	11.6997(5)	7.5733(16)	11.9955(7)	13.8856(3)	8.3806(3)
<i>b</i> /Å	21.5296(8)	7.5824(3)	8.7066(19)	10.9525(7)	15.5863(4)	13.3652(4)
<i>c</i> /Å	10.1015(4)	17.5946(7)	13.442(3)	12.7788(8)	12.3909(3)	9.0229(3)
α /deg	90	90	78.741(2)	90	90	90
β /deg	103.2029(6)	108.7288(6)	74.963(2)	94.2060(10)	92.948(2)	103.7934(4)
γ /deg	90	90	88.673(3)	90	90	90
<i>Z</i>	4	4	2	4	4	2
μ (MoK α)/mm ⁻¹	1.805	2.293	1.964	1.974	1.459	1.69
Max. and min. <i>Trans.</i>	0.746 and 0.678	0.746 and 0.656	0.746 and 0.638	0.746 and 0.643	0.926 and 0.655	0.752 and 0.551
2 θ _{max} /deg.	51.996	51.998	52.000	51.988	54.998	55.800
<i>R</i> ₁ [<i>I</i> > 2 σ (<i>I</i>)] on <i>F</i>	0.0223	0.0299	0.0376	0.0232	0.0486	0.0168
<i>wR</i> ₂ (all data) on <i>F</i> ²	0.0570	0.0865	0.0963	0.0600	0.0696	0.0445
Goodness-of-fit on <i>F</i> ²	1.030	1.045	1.006	1.033	1.027	1.064

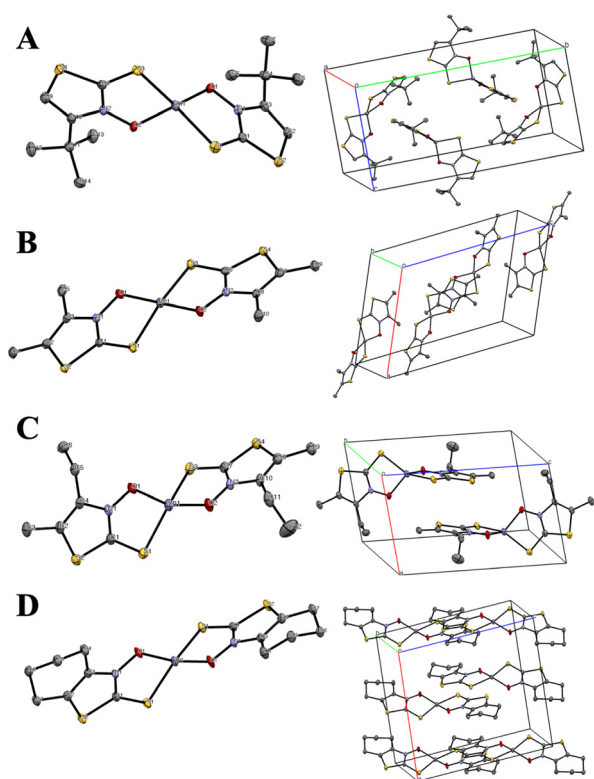


Fig. 5 Molecular structures with atomic numbering scheme (right side) and packing diagrams (left side) for (A) Zn(4)₂, (B) Zn(5f)₂, (C) Zn(5h)₂, and (D) Zn(6)₂. The thermal ellipsoids of non-H atoms are depicted at the 50% probability level. Hydrogen atoms are omitted for clarity.

activity. As these experiments were not conducted simultaneously, a direct comparison of the IC₅₀ values was not feasible. Thus, to compare these values more accurately, the relative IC₅₀ values were calculated using the IC₅₀ value of zinc sulfate—the reference material—for both the present and previous experiments. The calculated relative IC₅₀ values are presented in Table 3 for analysis and comparison. Zn(4)₂, Zn(5f)₂, Zn(5h)₂,

and Zn(6)₂, *i.e.*, the zinc(II) complexes having the alkyl-substituted 3,2-HTT ligands, were found to have more than 4-fold higher inhibitory activity than the previously reported Zn(1a)₂–Zn(1e)₂ and 10-fold higher inhibitory activity than Zn(2a)₂ and Zn(2f)₂. Zn(5f)₂ with a 3,2-HTT ligand with two methyl groups at the 4- and 5-positions was identified as the most potent among the 3,2-HTT-based zinc(II) complexes investigated. Thus, a complex with smaller and less hydrophobic functional groups on the 3,2-HTT skeleton exhibited the highest inhibitory activity, suggesting that the hydrophobicity and molecular size of the complexes affect the insulin-mimetic activity. Therefore, an attempt was made to quantify the partition coefficient (*log P* value), which is a lipophilic parameter of a compound and one of the most important measures in evaluating the pharmacokinetics of a drug, using reversed-phase high-performance liquid chromatography (HPLC). Among the 11 complexes exhibiting insulin-mimetic activity, Zn(4)₂, Zn(5f)₂, Zn(5h)₂, and Zn(6)₂ were soluble in conventional organic solvents, and their *log P* values were successfully determined; however, the *log P* values of other complexes with phenyl groups could not be determined, because of their low solubility in the HPLC mobile phase. The obtained *log P* values are presented in Table 3, all of which are <5 and satisfy Lipinski's Rule of Five, *i.e.*, *log P* < 5. However, these data are insufficient for meaningful comparisons. The calculated *log P* values (*C log P*) for the 11 complexes are also presented in Table 3. These results indicated that Zn(4)₂, Zn(5f)₂, Zn(5h)₂ and Zn(6)₂, which were estimated to be less hydrophobic than the complexes with phenyl groups, tended to exhibit higher insulin-mimetic activity.

Next, we focused on the size of the complexes, as the results in Table 3 indicated that smaller molecules had higher insulin-like activity. To examine the effect of the molecular size on the insulin-mimetic activity, Verloop's sterimol parameters (*L*, *B*₁, and *B*₅) of the ligand moiety of the complex were estimated. These parameters are frequently used in quantitative structure–activity relationship studies of bioactive materials to quantify and compare the steric bulkiness of different substituents



Table 2 Selected bond length (d) and bond angles (ω) for Zn(3)₂, Zn(4)₂, Zn(5f)₂, Zn(5h)₂, and Zn(6)₂

Bond	d [Å]					
	Zn(4) ₂	Zn(5f) ₂	Zn(5h) ₂	Zn(6) ₂	Zn(3) ₂ (with pyridine)	Zn(5f) ₂ (with pyridine)
Zn1–S1	2.2979 (5)	2.3258 (7)	2.3138(11)	2.3163 (5)	2.4121(6)	2.3747(4)
Zn1–S3	2.3104 (5)	2.3057 (7)	2.3191(11)	2.3163 (5)	2.3961(6)	2.3933(4)
Zn1–O1	1.9772 (12)	1.974 (2)	1.993(3)	1.9790 (14)	2.0758(13)	2.0857(11)
Zn1–O2	1.9984 (12)	1.9907 (19)	1.967(3)	1.9790 (14)	2.0492(14)	2.0892(11)
Bond angle	ω [°]					
	Zn(4) ₂	Zn(5f) ₂	Zn(5h) ₂	Zn(6) ₂	Zn(3) ₂ (with pyridine)	Zn(5f) ₂ (with pyridine)
O1–Zn1–O2	109.87 (5)	110.03 (8)	113.37(11)	102.62 (9)	165.18(6)	175.50(5)
O1–Zn1–S3	124.56 (4)	127.49 (6)	114.08(8)	129.51 (4)	91.42(4)	85.80(4)
O2–Zn1–S3	89.34 (3)	90.21 (6)	90.57(8)	89.92 (4)	86.28(4)	93.14(3)
S1–Zn1–O1	90.43 (3)	89.89 (6)	89.75(8)	89.92 (4)	84.98(4)	92.68(3)
S1–Zn1–O2	114.09 (4)	120.25 (6)	116.50(8)	129.51 (4)	89.48(4)	84.78(3)
S1–Zn1–S3	129.181 (17)	121.50 (3)	133.87(4)	118.96 (3)	149.12(2)	132.211(15)

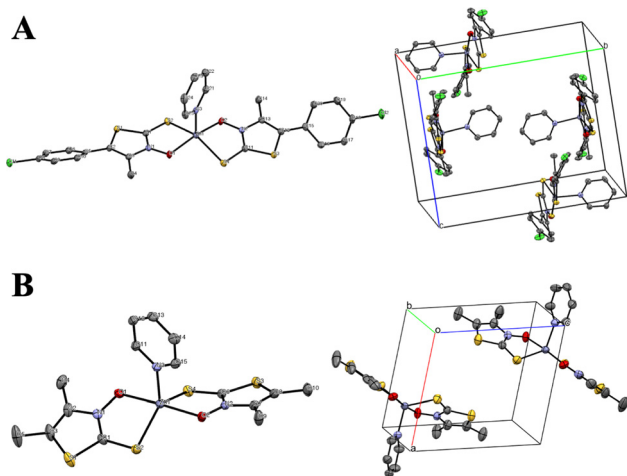


Fig. 6 Molecular structures with the atomic numbering scheme (right side) and packing diagrams (left side) for (A) Zn(3)₂ and (B) Zn(5f)₂ crystallized from pyridine-containing solvents. The thermal ellipsoids of non-H atoms are depicted at the 50% probability level.

attached to a molecule. The descriptors L , B_1 , and B_5 represent the length, minimum width, and maximum width of the substituents, respectively, and the estimated values are presented in Table 4. To examine the correlation between these parameters and insulin-like activity, we employed the pIC_{50} value—a commonly used index of inhibitory activity in structure–activity relationship studies of drug candidates—which is defined as follows:

$$\text{pIC}_{50} = -\log(\text{IC}_{50}).$$

The relative pIC_{50} values of the zinc(II) complexes with 3,2-HTT ligands against the pIC_{50} of zinc sulfate were plotted against the above descriptors, as shown in Fig S1 (ESI†). A negative correlation was observed between the relative pIC_{50} values and B_5 , and a weak negative correlation was observed with L . These results suggest that the molecular size affects the insulin-like activity, with smaller complexes tending to yield better results.

In addition to the lipophilicity and the molecular size, the stability constant ($\log \beta$) of the complexes is an important factor affecting insulin-mimetic activity, as it has been reported that high insulin-mimetic activity is observed in zinc(II) complexes

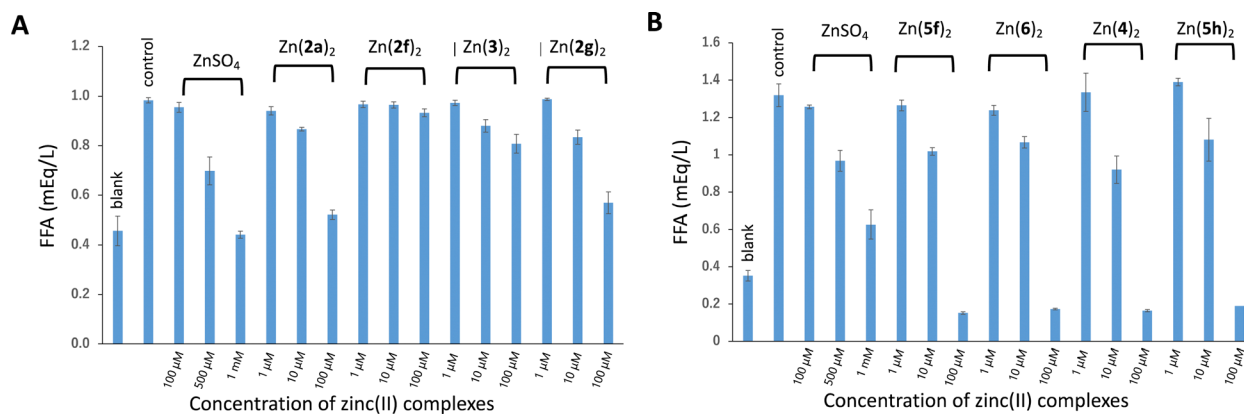


Fig. 7 Inhibitory effects of zinc(II) complexes on stimulated FFA release from rat adipocytes treated with epinephrine: (A) for Zn(2a)₂, Zn(2f)₂, Zn(2g)₂, and Zn(3)₂; (B) for Zn(4)₂, Zn(5f)₂, Zn(5h)₂, and Zn(6)₂. Each column represents the mean \pm standard deviation for three experiments. “Blank” refers to normal adipocyte, and “control” refers to epinephrine-stimulated rat adipocyte.



Table 3 *In vitro* insulin-mimetic activities, partition coefficients ($\log P$), and overall stability constants ($\log \beta$) for Zn(**2a**)₂, Zn(**2f**)₂, Zn(**4**)₂, Zn(**5f**)₂, Zn(**5h**)₂, and Zn(**6**)₂

Compound	IC ₅₀ /μM	Ratio ^a	pIC ₅₀ ^b	pIC _{50,rel} ^c	Log <i>P</i>	<i>C</i> Log <i>P</i>	Log β
Zn(2a) ₂	228	4.29	3.64	1.21		4.41	
Zn(2f) ₂	289	3.38	3.54	1.18		5.29	
Zn(4) ₂	19	60.9	4.73	1.61	4.34	3.37	14.40
Zn(5f) ₂	16	70.7	4.79	1.63	3.27	1.56	12.26
Zn(5h) ₂	21	55.5	4.69	1.59	2.21	2.08	12.76
Zn(6) ₂	24	47.6	4.62	1.60	2.57	1.85	12.10
ZnSO ₄	977 ^d	1	3.01 ^d	1			
	1,138 ^e		2.94 ^e				
Zn(1a) ₂	37 ^f	12.7 ^g	4.43	1.33		5.37	
Zn(1b) ₂	30 ^f	15.7 ^g	4.52	1.36		6.59	
Zn(1c) ₂	37 ^f	12.7 ^g	4.43	1.33		5.15	
Zn(1d) ₂	44 ^f	10.7 ^g	4.36	1.31		5.50	
Zn(1e) ₂	36 ^f	13.1 ^g	4.44	1.34		— ^h	

^a Relative insulin-mimetic activity index based on the IC₅₀ value of ZnSO₄ as a standard. ^b The ordinary logarithmic representation of IC₅₀ is defined as follows: pIC₅₀ = -log (IC₅₀). ^c Relative pIC₅₀ values of zinc(II) complexes against zinc sulfate. ^d Values obtained in the experiment shown in Fig. 7(A). ^e Value obtained in the experiment shown in Fig. 7(B). ^f Data were obtained from ref. 11. ^g These values were calculated using the IC₅₀ value of ZnSO₄ (0.47 mM) measured in the same experiment. ^h Because of the polarized electronic structure of the nitro groups, the calculated values were implausibly hydrophilic and were eliminated.

Table 4 Physicochemical parameters of the 3-hydroxythiazole-2(3H)-thiones (3,2-HTTs) studied

Compound	<i>L</i> ^a	<i>B</i> ₁ ^b	<i>B</i> ₃ ^c	p <i>K</i> _a
4	5.5303	2.1439	5.7094	5.64 ^d
5f	6.5525	1.8709	4.3106	4.78 ^d
5h	6.3156	1.8543	5.0319	4.91 ^d
6	6.3006	1.9235	5.7004	4.68 ^d
1a	5.1222	2.4933	7.1821	4.01 ^e
1b	5.1150	2.4699	8.2762	4.91 ^e
1c	5.1173	2.4726	9.0764	4.63 ^e
1d	5.1145	2.4677	7.6386	4.80 ^e
1e	5.1132	2.4733	8.5457	3.92

^a Total length of a ligand in bond direction. ^b Shortest distance from *L* axis when a ligand is projected on a plane perpendicular to *L*. ^c Longest distance from *L* axis when a ligand is projected on a plane perpendicular to *L*. ^d Each value was obtained by extrapolating a plot of the p*K*_a values measured in 40.0%, 50.0%, and 66.7% aqueous THF. ^e Data were obtained from ref. 11.

with $\log \beta$ values not exceeding 10.5, while the activity tends to be lower for complexes with $\log \beta$ exceeding 10.5.²⁸ Prior to studying the correlation between the stability constant of the complex and the insulin-mimetic activity, the acid dissociation constants (p*K*_a values), which are directly related to the stability of the complexes, of **4**, **5f**, **5h**, and **6** were quantified. Because the ligands are insoluble in water, the p*K*_a values were measured in a tetrahydrofuran (THF)–water binary solvent with various THF ratios, and the obtained values were plotted against the THF content (volume%) and extrapolated to estimate the p*K*_a value in 100% water.¹⁶ Other ligands could not be measured, because they were insoluble, even in this solvent. The p*K*_a values of **4**, **5f**, **5h**, and **6** were estimated to be within the range of 4.6–5.6, indicating that 3,2-HTTs are acidic and

comparable to acetic acid (Table 4). The disparity in the p*K*_a values of the ligands is attributed to the electron-donation strength of the alkyl groups. The stability constants ($\log \beta$ values) of Zn(**4**)₂, Zn(**5f**)₂, Zn(**5h**)₂, and Zn(**6**)₂ were determined using the Bjerrum method.^{29–32} All measurements were conducted in 50% THF, and the p*K*_a values of the corresponding ligands in 50% THF were used to calculate the $\log \beta$ values. The results are summarized in Table 3. The $\log \beta$ values of the four zinc complexes were in the range of 12–14. As reported by Irving and Rossotti,³³ the stability constant of metal complexes is approximately proportional to the p*K*_a value of the ligand measured under the same conditions. In addition, data reported by Mui *et al.* indicated a proportional relationship between the stability constants of metal complexes in organic solvents with varying water contents and the p*K*_a values of the ligands in the corresponding organic solvents with the same water content.³⁴ Considering these findings, the stability constants of the complexes Zn(**4**)₂, Zn(**5f**)₂, Zn(**5h**)₂, and Zn(**6**)₂ in water in this study were estimated to be approximately 8.7, 8.8, 10.4, and 9.0, respectively, satisfying the condition of <10.5.

Conclusions

We demonstrated that newly synthesized zinc(II) complexes with 4-alkylated and 4,5-dialkylated 3,2-HTT ligands exhibit higher insulin-like activity than those with 3,2-HTT ligands with phenyl substituents. Zn(**5f**)₂, which has two methyl groups at positions 4 and 5, is the most potent among the zinc(II) complexes with 3,2-HTT ligands synthesized to date. The lipophilicity and molecular size of the complexes were identified as factors exerting a degree of influence on the observed increase in activity. The experimental $\log P$ values of the complexes with alkylated ligands were <5. A comparison of the experimental $\log P$ and *C* $\log P$ values of the complexes with alkylated 3,2-HTT ligands suggested that the $\log P$ values for complexes with phenyl groups were >5. Thus, higher activity was observed for complexes with $\log P$ values of <5 owing to the smaller alkyl groups. Regarding the effect of the stability constant of the complex on the insulin-mimetic activity, the $\log \beta$ was maintained within a range not exceeding 10.5, strengthening the versatility of the guideline of the stability constants required for complexes that exhibit high insulin-mimetic activity. The relationship between the hydrophobicity and molecular size of the complexes and their insulin-mimetic activity has not been sufficiently clarified. Thus, the findings of this study provide valuable guidance for the development of more potent hypoglycemic zinc complexes.

Experimental

General

¹H-NMR spectra were recorded on an ECP-400 spectrometer (JEOL Ltd, Japan). Chemical shifts (δ) are reported in ppm using tetramethylsilane or an undeuterated solvent as internal standards in the deuterated solvent used. Coupling constants



(*J*) are given in Hz. ^{13}C -NMR spectra were recorded on an ECP-400 spectrometer (JEOL Ltd, Japan). Chemical shift multiplicities are reported as s = singlet, d = doublet, t = triplet, q = quintet, m = multiplet. Infrared (IR) spectra were obtained using FT/IR-4100, FT/IR-660plus, or FT/IR-460plus spectrophotometers (JASCO, Ltd, Japan). Fast-atom-bombardment (FAB) mass spectra were taken on a JMS-600-H mass spectrometer (JEOL Ltd, Japan). Xenon was used as a bombardment gas, and all analyses were carried out in positive mode with the ionization energy and the accelerating voltage set at 70 eV and 3 kV, respectively. A mixture of dithiothreitol (DTT) and α -thioglycerol (TG) (1 : 1) was used as a liquid matrix. All conventional chemicals used in the present study are commercially available and were used as received. Column chromatography was carried out on silica gel (particle size; 46–50 μM ; Fuji Silysia Chemical Ltd, Japan). Compounds **3**, **12–14**, **18**, and **19** were synthesized by the method reported in the literature cited in the main text.

Synthesis

2-Phenylacetaldehyde oxime (8a). To a suspension of 2-phenylacetaldehyde (**7a**, 1.99 g, 16.6 mmol) and hydroxylamine hydrochloride (1.16 g, 16.6 mmol) in 50% aqueous methanol (12 mL), an aqueous solution of sodium carbonate (881 mg, 8.31 mmol) was slowly added. The resulting mixture was stirred at room temperature for 2.5 h, and then methanol was evaporated. H_2O (20 mL) was added to the reaction mixture followed by extraction with Et_2O (3×50 mL). The organic phase was dried over sodium sulfate. After evaporation of the solvent, the resulting pale-yellow residue was purified by column chromatography on silica gel with *n*-hexane/ethyl acetate (4/1, v/v) as eluents to give **8a** as a white solid (1.23 g, 55%). ^1H NMR (chloroform-*d*, 400 MHz; a mixture of *E*- and *Z*-isomer) δ /ppm 3.54 (d, 2H, *J* = 6.1 Hz, *Z*-isomer), 3.75 (d, 2H, *J* = 5.3 Hz, *E*-isomer), 6.90 (t, 1H, *J* = 5.3 Hz, *E*-isomer), 7.21–7.35 (m, 10H, *E*- and *Z*-isomer), 7.54 (t, 1H, *J* = 6.1 Hz, *Z*-isomer). ^{13}C NMR (chloroform-*d*, 100 MHz) δ /ppm 31.8, 36.0, 126.8, 127.0, 128.9, 128.9, 128.9, 136.2, 136.7, 150.8, 151.0. The spectroscopic data for this compound are consistent with data available in the literature.³⁵

2-(*p*-Tolyl)acetaldehyde oxime (8f). Hydroxylamine hydrochloride (317 mg, 4.57 mmol) was added to a solution of 2-(*p*-tolyl)acetaldehyde (**7f**, 670 mg, 3.76 mmol) in methanol (15 mL) followed by pyridine (0.30 mL, 3.79 mmol). The mixture was refluxed for 2 h. After evaporation of the solvent, H_2O (20 mL) was added to the reaction mixture followed by extraction with dichloromethane (2×20 mL). The organic phase was washed with 1.0 M HCl (13 mL), and then dried over sodium sulfate. After evaporation of the solvent, the resulting pale yellow residue was purified by column chromatography on silica gel with *n*-hexane/ethyl acetate (4/1, v/v) as eluents to give **8f** as a white solid (407 mg, 56%). ^1H NMR (chloroform-*d*, 400 MHz; a mixture of *E*- and *Z*-isomer) δ /ppm 2.33 (s, 6H, *E*- and *Z*-isomer), 3.49 (d, 2H, *J* = 6.2 Hz, *Z*-isomer), 3.70 (d, 2H, *J* = 5.2 Hz, *E*-isomer), 6.89 (t, 1H, *J* = 5.2 Hz, *E*-isomer), 7.09–7.14 (m, 8H, *E*- and *Z*-isomer), 7.52 (t, 1H, *J* = 6.2 Hz, *Z*-isomer). ^{13}C NMR (chloroform-*d*, 100 MHz) δ /ppm 21.10, 31.22, 128.7, 128.8,

129.5, 133.6, 136.3, 151.5. The spectroscopic data for this compound are consistent with data available in the literature.³⁶

2-(4-Bromophenyl)acetaldehyde oxime (8g). This material was prepared from **7g** (871 mg, 4.37 mmol) with hydroxylamine hydrochloride (370 mg, 5.33 mmol) in a procedure analogous to that for obtaining **8f**. The product was obtained as a white solid (468 mg, 41%). ^1H NMR (chloroform-*d*, 400 MHz; a mixture of *E*- and *Z*-isomer) δ /ppm 3.48 (d, 2H, *J* = 6.1 Hz, *Z*-isomer), 3.68 (d, 2H, *J* = 5.4 Hz, *E*-isomer), 6.85 (t, 1H, *J* = 5.4 Hz, *E*-isomer), 6.94 (s, 1H, OH), 7.07 (s, 1H, OH), 7.10 (d, 4H, *J* = 7.9 Hz, *E*- and *Z*-isomer), 7.44 (d, 4H, *J* = 7.9 Hz, *E*- and *Z*-isomer), 7.49 (t, 1H, *J* = 6.1 Hz, *Z*-isomer). ^{13}C NMR (chloroform-*d*, 100 MHz) δ /ppm 31.01, 35.33, 130.6, 130.6, 131.9, 131.9, 150.3. The spectroscopic data for this compound are consistent with data available in the literature.³⁷

2-Phenylacetaldehyde *O*-(*tert*-butyldimethylsilyl)oxime (9a). To a solution of **8a** (1.23 g, 9.14 mmol) and *tert*-butylchlorodimethylsilane (2.09 g, 13.9 mmol) in dichloromethane (20 mL), imidazole (1.25 g, 18.4 mmol) was slowly added at 0 $^\circ\text{C}$. The resulting mixture was stirred at room temperature for 4 h. H_2O (100 mL) was added to the reaction mixture, and the organic materials were extracted with chloroform (2×100 mL). The organic phase was dried over sodium sulfate. After evaporation of the solvent, the resulting pale yellow residue was purified by column chromatography on silica gel with *n*-hexane/ethyl acetate (9/1, v/v) as eluents to give **9a** as a pale yellow liquid (2.16 g, 94%). ^1H NMR (chloroform-*d*, 400 MHz; a mixture of *E*- and *Z*-isomer) δ /ppm 0.18 (s, 6H, *Z*-isomer), 0.21 (s, 6H, *E*-isomer), 0.9 (s, 9H, *Z*-isomer), 0.96 (s, 9H, *E*-isomer), 3.53 (d, 2H, *J* = 6.4 Hz, *Z*-isomer), 3.74 (d, 2H, *J* = 5.2 Hz, *E*-isomer), 7.02 (t, 1H, *J* = 5.2 Hz, *E*-isomer), 7.20–7.33 (m, 10H, *E*- and *Z*-isomer), 7.58 (t, 1H, *J* = 6.4 Hz, *Z*-isomer). ^{13}C NMR (chloroform-*d*, 100 MHz) δ /ppm 18.3, 25.8, 26.2, 126.6, 128.8, 128.9, 137.2, 154.2. This material was used directly in the next step without further purification.

3-hydroxy-5-phenylthiazole-2(3*H*)-thione (2a) (via 10a and 11a). To a slurry of **9a** (2.16 g, 8.67 mmol) and *N*-bromosuccinimide (1.55 g, 8.71 mmol) in tetrachloromethane (40 mL), 2,2'-azodiisobutyronitrile (83.7 mg, 0.588 mmol) was slowly added. The mixture was then refluxed for 3 h. After cooling to room temperature, the reaction mixture was passed through a filter and the filtrate was washed successively with a 10% sodium thiosulfate solution (50 mL) and water (2×50 mL), and the organic phase was dried over sodium sulfate. After evaporation of the solvent, **10a** was obtained as an orange oily material (3.10 g). This material was directly used in the next step without further purification. ^1H NMR (chloroform-*d*, 400 MHz; a mixture of *E*- and *Z*-isomer) δ /ppm 0.15 (s, 6H, *E*-isomer), 0.17 (s, 6H, *Z*-isomer), 0.92 (s, 9H, *E*-isomer), 0.92 (s, 9H, *Z*-isomer), 5.70 (d, 1H, *J* = 8.9 Hz, *E*-isomer), 6.29 (d, 1H, *J* = 7.7 Hz, *Z*-isomer), 7.30–7.47 (m, 10H, *E*- and *Z*-isomer), 7.42 (d, 1H, *J* = 7.7 Hz, *Z*-isomer) 7.92 (d, 1H, *J* = 8.9 Hz, *E*-isomer). ^{13}C NMR (chloroform-*d*, 100 MHz) δ /ppm 18.2, 18.3, 26.0, 26.1, 40.3, 48.6, 127.9, 128.1, 128.8, 128.9, 129.0, 138.0, 138.1, 152.7, 153.4. To a slurry of potassium *O*-ethylthiocarbonate (1.47 g, 9.18 mmol) in acetone (45 mL) was added a solution of **10a** (3.00 g, 9.16 mmol) over a



period of 15 min at room temperature. The reaction mixture was stirred for 26 h at room temperature. After evaporation of the solvent, H₂O (50 mL) was added to the residue, and organic materials were extracted with ethyl acetate (3 × 50 mL). The combined organic phase was dried over sodium sulfate. After evaporation of the solvent, **11a** was obtained as an orange liquid (4.77 g). This material was directly used in the next step without further purification. ¹H NMR (chloroform-d, 400 MHz; a mixture of *E*- and *Z*-isomer) δ/ppm 0.16 (s, 6H, *Z*-isomer), 0.16 (s, 6H, *E*-isomer), 0.89 (s, 9H, *Z*-isomer), 0.91 (s, 9H, *E*-isomer), 1.33–1.44 (m, 6H, *E*- and *Z*-isomer), 4.56–4.68 (m, 4H, *E*- and *Z*-isomer), 5.58 (d, 1H, *J* = 6.5 Hz, *E*-isomer), 6.15 (d, 1H, *J* = 6.7 Hz, *Z*-isomer), 7.21 (d, 1H, *J* = 6.7 Hz, *Z*-isomer), 7.29–7.35 (m, 10H, *E*- and *Z*-isomer), 7.71 (d, 1H, *J* = 6.5 Hz, *E*-isomer). ¹³C NMR (chloroform-d, 100 MHz) δ/ppm 13.7, 13.8, 18.1, 18.3, 25.9, 26.1, 52.7, 53.9, 128.0, 128.2, 128.3, 128.5, 128.9, 136.2, 136.4, 152.2, 152.7, 211.2, 211.5. Zinc chloride (6.04 g, 47.1 mmol) was added to a solution of **11a** (4.77 g, 12.9 mmol) in diethyl ether (30 mL, anhydrous) at such a rate that the solvent did not boil constantly, and then the mixture was stirred for 8 days at room temperature. 1.0 M HCl (21 mL) was added dropwise to the mixture, and then the reaction mixture was stirred for 30 min at 0 °C to room temperature. The solution was filtered and the filtrate was extracted with chloroform (3 × 60 mL). The organic phase was dried over sodium sulfate. After evaporation of the solvent, the resulting brown residue was purified by column chromatography on silica gel with chloroform/ethyl acetate (1/1, v/v) as eluents to give **2a** as a brown solid (282 mg, 29%). ¹H NMR (chloroform-d, 400 MHz) δ/ppm 7.18 (s, 1H), 7.30–7.40 (m, 5H). ¹³C NMR (chloroform-d, 100 MHz) δ/ppm 115.6, 119.5, 124.9, 125.2, 128.4, 129.2, 130.6. IR (KBr): 3126 (ν_{C-H}), 1647 (ν_{C=S}), 1509 (ν_{N-O}), 1348 (ν_{N-O}), and 756 cm⁻¹ (δ_{C-H}). Anal. calcd for C₉H₇NOS₂·0.2H₂O: C, 50.77; H, 3.50; N, 6.58%. Found: C, 50.81; H, 3.28; N, 6.54%.

2-(*p*-Tolyl)acetaldehyde *O*-(*tert*-butyldimethylsilyl) oxime (9f). This material was prepared from **8f** (643 mg, 4.31 mmol) with *tert*-butylchlorodimethylsilane (979 mg, 6.49 mmol) in a procedure analogous to that for obtaining **9a**. The product (**9f**) was obtained as pale-yellow oily material (908 mg, 80%). ¹H NMR (chloroform-d, 400 MHz; a mixture of *E*- and *Z*-isomer) δ/ppm 0.18 (s, 6H, *Z*-isomer), 0.20 (s, 6H, *E*-isomer), 0.94 (s, 9H, *Z*-isomer), 0.96 (s, 9H, *E*-isomer), 2.32 (s, 6H, *E*- and *Z*-isomer), 3.48 (d, 2H, *J* = 6.4 Hz, *Z*-isomer), 3.69 (d, 2H, *J* = 5.1 Hz, *E*-isomer), 6.99 (t, 1H, *J* = 5.1 Hz, *E*-isomer), 7.08–7.13 (m, 8H, *E*- and *Z*-isomer), 7.55 (t, 1H, *J* = 6.4 Hz, *Z*-isomer). ¹³C NMR (chloroform-d, 100 MHz) δ/ppm 18.24, 21.10, 26.18, 31.79, 35.64, 128.7, 129.4, 134.1, 136.1, 154.2, 154.6. This material was used directly in the next step without further purification.

3-Hydroxy-5-(*p*-tolyl)thiazole-2(3*H*)-thione (2f) (via 10f and 11f). Bromide **10f** (2.28 g, orange oily material) was prepared from **9f** (665 mg, 2.02 mmol) with *N*-bromosuccinimide (388 mg, 2.18 mmol) and 2,2'-azodiisobutyronitrile (20.9 mg, 0.127 mmol) in a procedure analogous to that for obtaining **10a**, and was directly used in the next step without further purification. ¹H NMR (chloroform-d, 400 MHz; a mixture of *E*- and *Z*-isomer) δ/ppm 0.15 (s, 6H, *E*-isomer), 0.17 (s, 6H, *Z*-isomer), 0.92 (s, 9H, *E*-isomer), 0.93 (s, 9H, *Z*-isomer), 2.34 (s, 6H, *E*- and *Z*-isomer),

5.69 (d, 1H, *J* = 9.0 Hz, *E*-isomer), 6.28 (d, 1H, *J* = 7.7 Hz, *Z*-isomer), 7.17 (d, 2H, *J* = 7.7 Hz, *E*-isomer), 7.34 (d, 2H, *J* = 7.7 Hz, *E*-isomer), 7.38 (d, 1H, *J* = 7.7 Hz, *Z*-isomer), 7.22 (d, 2H, *J* = 7.6 Hz, *Z*-isomer), 7.42 (d, 2H, *J* = 7.6 Hz, *Z*-isomer), 7.93 (d, 1H, *J* = 9.0 Hz, *E*-isomer). ¹³C NMR (chloroform-d, 100 MHz) δ/ppm 18.21, 21.28, 26.05, 40.29, 48.69, 127.7, 127.9, 129.7, 135.2, 139.0, 152.7, 153.4. The obtained crude **10f** (2.28 g, 6.66 mmol (crude), orange oily material) was converted into **11f** (brown liquid, 2.55 g) by reacting with *O*-ethylthiocarbonate (1.11 g, 6.94 mmol) in acetone (48 mL) using the same procedure that for obtaining **11a**. The obtained **11f** was directly used in the next step without further purification; ¹H NMR (chloroform-d, 400 MHz; a mixture of *E*- and *Z*-isomer) δ/ppm 0.16 (s, 6H, *E*-isomer), 0.17 (s, 6H, *Z*-isomer), 0.90 (s, 9H, *Z*-isomer), 0.92 (s, 9H, *E*-isomer), 1.36–1.44 (m, 6H, *E*- and *Z*-isomer), 2.33 (s, 6H, *E*- and *Z*-isomer), 4.57–4.66 (m, 4H, *E*- and *Z*-isomer), 5.54 (d, 1H, *J* = 6.6 Hz, *E*-isomer), 6.13 (d, 1H, *J* = 6.9 Hz, *Z*-isomer), 7.19 (d, 1H, *J* = 6.9 Hz, *Z*-isomer), 7.11–7.31 (m, 8H, *E*- and *Z*-isomer), 7.71 (d, 1H, *J* = 6.6 Hz, *Z*-isomer). ¹³C NMR (chloroform-d, 100 MHz) δ/ppm 18.96, 23.28, 23.45, 26.40, 31.15, 31.32, 52.98, 57.59, 75.31, 133.3, 133.6, 133.9, 134.8, 138.2, 138.5, 143.0, 143.3, 157.5, 158.0. Ligand **2f** was then prepared by reacting the crude **11f** (1.14 g, 2.96 mmol) with zinc chloride (4.10 g, 2.99 mmol) in diethyl ether (5 mL, anhydrous) in a procedure analogous to that for obtaining **2a**, and obtained as a gray solid (285 mg, 19%, 3 steps). ¹H NMR (dimethyl sulfoxide-d₆, 400 MHz) δ/ppm 2.30 (s, 3H), 7.20 (d, 2H, *J* = 8.0 Hz), 7.34 (d, 2H, *J* = 8.0 Hz) 11.6 (s, 1H). ¹³C NMR (dimethyl sulfoxide-d₆, 100 MHz) δ/ppm 21.28, 112.1, 121.8, 124.6, 128.7, 130.1, 137.6, 165.1. IR (KBr): 3159 (ν_{C-H}), 1663 (ν_{C=S}), 1508 (ν_{N-O}), 1414 (ν_{N-O}), and 780 cm⁻¹ (δ_{C-H}). HR-ESIMS calcd for C₁₀H₁₀NOS₂⁺ [M + H]⁺ 224.0198. Found 224.0227.

Synthesis of 2-(4-bromophenyl)acetaldehyde *O*-(*tert*-butyldimethylsilyl) oxime (9g)

This material was prepared from **8g** (468 mg, 2.19 mmol) with *tert*-butylchlorodimethylsilane (687 mg, 4.56 mmol) in a procedure analogous to that for obtaining **9a**. The product (**9g**) was obtained as a pale-yellow oily material (665 mg, 93%). ¹H NMR (chloroform-d, 400 MHz; a mixture of *E*- and *Z*-isomer) δ/ppm 0.17 (s, 6H, *Z*-isomer), 0.20 (s, 6H, *E*-isomer), 0.93 (s, 9H, *Z*-isomer), 0.95 (s, 9H, *E*-isomer), 3.47 (d, 2H, *J* = 6.4 Hz, *Z*-isomer), 3.68 (d, 2H, *J* = 5.2 Hz, *E*-isomer), 6.97 (t, 1H, *J* = 5.2 Hz, *E*-isomer), 7.07 (d, 2H, *J* = 8.0 Hz, *Z*-isomer), 7.08 (d, 2H, *J* = 8.0 Hz, *E*-isomer), 7.43 (d, 4H, *J* = 8.0 Hz, *E*- and *Z*-isomer), 7.56 (t, 1H, *J* = 6.4 Hz, *Z*-isomer). ¹³C NMR (chloroform-d, 100 MHz) δ/ppm 18.23, 26.08, 31.60, 65.55, 120.0, 130.8, 131.7, 136.6, 153.5. This material was used directly in the next step without further purification.

5-(4-Bromophenyl)-3-hydroxythiazole-2(3*H*)-thione (2g) (via 10g and 11g). Bromide **10g** was prepared from **8g** (665 mg, 2.02 mmol) with *N*-bromosuccinimide (388 mg, 2.18 mmol) and 2,2'-azodiisobutyronitrile (20.9 mg, 0.127 mmol) in a procedure analogous to that for obtaining **8f**. The product (**9g**) was obtained as an orange oily material (1.09 g). This crude material was directly used in the next step without further purification; ¹H NMR (chloroform-d, 400 MHz; a mixture of *E*- and *Z*-isomer)



δ /ppm 0.17 (s, 6H, *E*-isomer), 0.19 (s, 6H, *Z*-isomer), 0.91 (s, 9H, *E*-isomer), 0.92 (s, 9H, *Z*-isomer), 2.17 (s, 6H, *E* and *Z*-isomer), 5.64 (d, 1H, $J = 8.5$ Hz, *E*-isomer), 6.23 (d, 1H, $J = 7.5$ Hz, *Z*-isomer), 7.32 (d, 2H, $J = 8.2$ Hz, *E*-isomer), 7.33 (d, 2H, $J = 8.2$ Hz, *Z*-isomer), 7.36 (d, 1H, $J = 7.5$ Hz, *Z*-isomer), 7.50 (d, 4H, $J = 8.2$ Hz, *E*- and *Z*-isomer) 7.86(d, 1H, $J = 8.5$ Hz, *E*-isomer). ^{13}C NMR (chloroform-*d*, 100 MHz) δ /ppm 23.45, 16.52, 31.28, 45.42, 53.92, 133.0, 134.9, 140.4, 144.3, 157.9, 158.6. From the obtained crude **10g** (1.09 g, 2.67 mmol), **11g** was prepared using potassium *O*-ethylthiocarbonate (478 mg, 2.98 mmol) in a procedure analogous to that for obtaining **10a**, and was obtained as a yellow oil (908 mg). This material was directly used in the next step without further purification; ^1H NMR (chloroform-*d*, 400 MHz; a mixture of *E*- and *Z*-isomer) δ /ppm 0.15 (s, 6H, *E*-isomer), 0.16 (s, 6H, *Z*-isomer), 0.91 (s, 9H, *Z*-isomer), 0.92 (s, 9H, *E*-isomer), 1.38 (t, 6H, $J = 7.0$ Hz, *E*- and *Z*-isomer), 4.59–4.65 (m, 4H, *E*- and *Z*-isomer), 5.53 (d, 1H, $J = 6.2$ Hz, *E*-isomer), 6.09 (d, 1H, $J = 6.6$ Hz, *Z*-isomer), 7.17 (d, 1H, $J = 6.6$ Hz, *Z*-isomer), 7.22–7.24 (m, 4H, *E*- and *Z*-isomer), 7.45–7.50 (m, 4H, *E*- and *Z*-isomer), 7.68 (d, 1H, $J = 6.2$ Hz, *E*-isomer). ^{13}C NMR (chloroform-*d*, 100 MHz) δ /ppm 13.77, 14.28, 18.25, 21.13, 25.92, 26.09, 47.65, 52.25, 60.47, 70.36, 122.2, 122.9, 130.3, 131.9, 132.0, 135.7, 151.6, 151.9. Ligand **2g** was then prepared by reacting the crude **11g** (343 mg, 0.764 mmol) with zinc chloride (519 mg, 3.81 mmol) in diethyl ether (10 mL, anhydrous) in a procedure analogous to that for obtaining **2a**, and obtained as a gray solid (124 mg, 45%, 3 steps). ^1H NMR (dimethyl sulfoxide-*d*₆, 400 MHz) δ /ppm. 7.41 (d, 2H, $J = 8.3$ Hz), 7.58 (d, 2H, $J = 8.3$ Hz), 7.98 (s, 1H), 11.64 (s, 1H). ^{13}C NMR (dimethyl sulfoxide-*d*₆, 100 MHz) δ /ppm 110.7, 120.9, 123.3, 126.6, 130.9, 132.4, 165.1. IR (KBr): 3087 ($\nu_{\text{C-H}}$), 1653 ($\nu_{\text{C=S}}$), 1474 ($\nu_{\text{N-O}}$), 1401 ($\nu_{\text{N-O}}$), and 768 cm^{-1} ($\delta_{\text{C-H}}$). ESIMS calcd for $\text{C}_9\text{H}_5^{79}\text{BrNS}_2$ [$\text{M} - \text{OH}$] $^-$: 269.9052 and $\text{C}_9\text{H}_5^{81}\text{BrNS}_2$ [$\text{M} - \text{OH}$] $^-$: 271.9031. Found: 269.9615 and 271.9545, respectively. Anal. calcd for $\text{C}_9\text{H}_6\text{BrNOS}_2 \cdot 0.25\text{EtOAc}$: C, 38.72; H, 2.60; N, 4.52%. Found: C, 38.88; H, 2.32; N, 4.98%.

Bis[3-hydroxy-5-phenylthiazole-2(3*H*)-thionolato]zinc(II): Zn(2a)₂.

To a solution of **2a** (23.7 mg, 134 μmol) in 50% aqueous ethanol (2 mL) was successively added LiOH \cdot 2H₂O (5.4 mg, 129 μmol) and a solution of Zn(OAc)₂ \cdot 2H₂O (14.7 mg, 67.0 μmol) in H₂O (1.0 mL). The mixture was then stirred at room temperature for 1 hour. The resulting precipitate was collected by filtration and washed with H₂O and THF to give Zn(2a)₂ as a white solid (16.6 mg, 34.6 μmol , 52%). ^1H NMR (dimethyl sulfoxide-*d*₆, 400 MHz) δ /ppm 7.24 (t, 1H, $J = 7.3$ Hz), 7.36 (dd, 2H, $J = 7.3, 7.6$ Hz), 7.45 (d, 2H, $J = 7.6$ Hz), 7.89 (s, 1H). ^{13}C NMR (dimethyl sulfoxide-*d*₆, 100 MHz) δ /ppm 110.9, 123.9, 124.6, 127.6, 129.5, 132.0, 165.2. IR (KBr): 3076 ($\nu_{\text{C-H}}$), 1579 ($\nu_{\text{C=S}}$), 1491 ($\nu_{\text{N-O}}$), 1363 ($\nu_{\text{N-O}}$), and 750 cm^{-1} ($\delta_{\text{C-H}}$). Anal. calcd for $\text{C}_{18}\text{H}_{12}\text{N}_2\text{O}_2\text{S}_4\text{Zn} \cdot 1.6\text{H}_2\text{O}$: C, 42.32; H, 3.00; N, 5.49% found: C, 42.14; H, 2.80; N, 5.35%.

Bis[3-hydroxy-5-(*p*-tolyl)thiazole-2(3*H*)-thionolato]zinc(II): Zn(2f)₂.

The complex Zn(2f)₂ was prepared from **11f** (48.0 mg, 0.215 mmol) with Zn(OAc)₂ \cdot 2H₂O (18.2 mg, 82.9 μmol) in a procedure analogous to that used for the preparation of Zn(2a)₂, with the exception that the reaction time was 3 hours. Zn(2f)₂ was obtained as white solid (28.1 mg, 55.4 μmol , 67%). ^1H NMR (dimethyl sulfoxide-*d*₆,

400 MHz) δ /ppm 2.29 (s, 3H), 7.18 (d, 2H, $J = 7.9$ Hz), 7.35 (d, 2H, $J = 7.9$ Hz), 7.88 (s, 1H). ^{13}C NMR (dimethyl sulfoxide-*d*₆, 100 MHz) δ /ppm 21.26, 110.9, 124.1, 123.3, 124.5, 129.1, 130.1, 137.0, 164.7. IR (KBr): 3087 ($\nu_{\text{C-H}}$), 1575 ($\nu_{\text{C=S}}$), 1508 ($\nu_{\text{N-O}}$), 1410 ($\nu_{\text{N-O}}$), and 783 cm^{-1} ($\delta_{\text{C-H}}$). Anal. calcd for $\text{C}_{20}\text{H}_{16}\text{N}_2\text{O}_2\text{S}_4\text{Zn} \cdot 0.3\text{H}_2\text{O}$: C, 46.60; H, 3.25; N, 5.44%. Found: C, 46.68; H, 3.49; N, 5.14%.

Bis[5-(4-bromophenyl)-3-hydroxythiazole-2(3*H*)-thionolato]zinc(II): Zn(2g)₂. The complex Zn(2g)₂ was prepared by reacting **11g** (123.8 mg, 0.430 mmol) with Zn(OAc)₂ \cdot 2H₂O (47.5 mg, 0.216 mmol) in 75% aqueous ethanol (4.0 mL) at room temperature for 3 h using the same procedure as that used for the preparation of Zn(2a)₂. Zn(2g)₂ was obtained as a white solid. ^1H NMR (dimethyl sulfoxide-*d*₆, 400 MHz) δ /ppm 7.42 (d, 2H, $J = 8.4$ Hz), 7.55 (d, 2H, $J = 8.4$ Hz), 8.04 (s, 1H). ^{13}C NMR (dimethyl sulfoxide-*d*₆, 100 MHz) δ /ppm 109.3, 120.2, 124.7, 126.4, 131.2, 132.4, 165.1. IR (KBr): 3089 ($\nu_{\text{C-H}}$), 1586 ($\nu_{\text{C=S}}$), 1486 ($\nu_{\text{N-O}}$), 1408 ($\nu_{\text{N-O}}$), and 797 cm^{-1} ($\delta_{\text{C-H}}$). Anal. calcd for $\text{C}_{18}\text{H}_{10}\text{Br}_2\text{N}_2\text{O}_2\text{S}_4\text{Zn} \cdot 0.7\text{H}_2\text{O}$: C, 33.14; H, 1.76; N, 4.30%. Found: C, 33.00; H, 2.05; N, 4.13%.

Bis[5-(4-chlorophenyl)-3-hydroxy-4-methylthiazole-2(3*H*)-thionolato]zinc(II): Zn(3)₂. The complex Zn(3)₂ was prepared from **3** (51.1 mg, 198 μmol) with Zn(ClO₄)₂ \cdot 6H₂O (35.9 mg, 97.0 μmol) in a procedure analogous to that used for the preparation of Zn(2a)₂, with the exception that lithium hydroxide was absent. Zn(3)₂ was obtained as a white solid (41.9 mg, 72.4 μmol , 75%). ^1H NMR (dimethyl sulfoxide-*d*₆, 400 MHz) δ /ppm 2.42 (s, 3H, CH₃), 7.54 (d, 2H, $J = 8.4$ Hz), 7.58 (d, 2H, $J = 8.4$ Hz). ^{13}C NMR (dimethyl sulfoxide-*d*₆, 100 MHz) δ /ppm 13.66, 118.3, 129.8, 130.0, 130.1, 133.9, 146.4, 164.4. Anal. calcd for $\text{C}_{18}\text{H}_{12}\text{N}_2\text{O}_2\text{S}_4\text{Zn}$: C, 41.50; H, 2.44; N, 4.84%. Found: C, 41.46; H, 2.63; N, 4.80%.

1-Chloro-3,3-dimethylbutan-2-one oxime (12). Hydroxylamine hydrochloride (2.21 g, 31.8 mmol) and sodium acetate (2.41 g, 29.4 mmol) were dissolved in water (9 mL), and 1-chloro-3,3-dimethylbutan-2-one (3.00 g, 22.3 mmol) was added to the aqueous solution with stirring. The resulting mixture was stirred vigorously for 20 minutes at room temperature, and then stirring was continued for 20 hours at room temperature. Ethyl acetate was added to the reaction mixture and organic materials were separated. The organic phase was dried over sodium sulfate. After evaporation of the solvent, **12** was obtained as a white solid (2.95 g, crude, 89%). This material was directly used in the next step without further purification. ^1H -NMR (chloroform-*d*, 400 MHz): δ /ppm, 1.21 (9H, s), 4.15 (2H, s), 8.24 (1H, br, OH). The spectral data were in good accordance with those reported previously.³⁸

3-Chlorobutan-2-one oxime (13). The oxime **13** was prepared from 3-chloro-2-butanone (5.00 g, 46.9 mmol) with hydroxylamine hydrochloride (3.56 g, 51.2 mmol) and sodium acetate (4.10 g, 50.0 mmol) in a procedure analogous to that for obtaining **12**, with the exception that the reaction mixture was allowed to stand at -20 °C for 19 hours after the initial vigorous stirring at room temperature for 20 min, and then again stirred vigorously for 20 minutes at room temperature. The product (**13**) was obtained as a colorless oil (5.45 g, 96%). ^1H -NMR (chloroform-*d*, 400 MHz): δ /ppm, 1.65 (3H, d, $J = 6.8$ Hz), 1.98 (3H, s), 4.62 (1H, q, $J = 6.8$ Hz), 8.02 (1H, br, OH).



The spectral data were in good accordance with those reported previously.¹⁷

O-Ethyl S-(2-(hydroxyimino)-3,3-dimethylbutyl) carbonodithioate (15). To a suspension of potassium *O*-ethylthiocarbonate (432 mg, 2.70 mmol) in acetone (6 mL) was added a solution of 1-chloro-3,3-dimethylbutan-2-one oxime (356 mg, 2.38 mmol) and acetone (6 mL) over a period of 30 min at room temperature. The reaction mixture was stirred for 3 hours at room temperature. The resulting solution was filtered through a Celite bed, and the filtrate was concentrated under reduced pressure. Water (15 mL) was added to the resulting residue, and organic materials were extracted with chloroform (3 × 10 mL). The organic phase was dried over sodium sulfate. After evaporation of the solvent, the resulting yellow residue was purified by column chromatography on silica gel with *n*-hexane/ethyl acetate (3/1, v/v) as eluents to give **15** as a white solid (492 mg, 88%). ¹H-NMR (chloroform-d, 400 MHz): δ/ppm, 1.18 (9H, s), 1.43 (3H, t, *J* = 7.2 Hz), 4.10 (2H, s), 4.68 (2H, q, *J* = 7.2 Hz). ¹³C NMR (chloroform-d, 100 MHz): δ/ppm, 13.9, 27.6, 29.1, 37.5, 70.4, 162.0, 214.7. HR-ESIMS calcd for C₉H₁₇NNaO₂S₂⁺ [M + Na]⁺ 258.0593. Found 258.0564.

O-Ethyl S-(3-(hydroxyimino)butan-2-yl) carbonodithioate (16). The xanthate **16** was prepared from **13** (135 mg, 1.11 mmol) with potassium *O*-ethylthiocarbonate (180 mg, 1.12 mmol) in a procedure analogous to that for obtaining **15**, with the exception that the reaction mixture was 19.5 hours. The product (**16**) was obtained as a yellow oil (153 mg, 66%). ¹H-NMR (chloroform-d, 400 MHz): δ/ppm, 1.42 (3H, t, *J* = 7.1 Hz), 1.51 (3H, d, *J* = 7.2 Hz), 1.94 (3H, s), 4.50 (1H, q, *J* = 7.2 Hz), 4.65 (2H, d, *J* = 7.1 Hz). The spectral data were in good accordance with those reported previously.¹⁷

Synthesis of O-ethyl S-(3-(hydroxyimino)pentan-2-yl) carbonodithioate (20). Hydroxylamine hydrochloride (1.10 g, 15.8 mmol) was added to a solution of *O*-ethyl S-(3-oxopentan-2-yl)carbonodithioate (2.70 g, 13.1 mmol) in methanol (7 mL) followed by addition of pyridine (1.3 mL, 16.3 mmol). The mixture was stirred for 11 hours at room temperature. After evaporation of the solvent, water (20 mL) and 4 M HCl aq. (20 mL) were added to the reaction mixture, and organic materials were extracted with ether (50 mL). The organic phase was dried over sodium sulfate. After evaporation of the solvent, the resulting pale-yellow residue was purified by column chromatography on silica gel with *n*-hexane/ethyl acetate (5/1, v/v) as eluents to give **20** as a white solid (1.12 g, 39%). ¹H-NMR (chloroform-d, 400 MHz): δ/ppm, 1.16 (3H, t, *J* = 7.6 Hz), 1.43 (3H, t, *J* = 7.1 Hz), 1.54 (3H, d, *J* = 7.1 Hz), 2.43 (2H, dq, *J* = 13.4, 7.6 Hz), 4.54 (1H, q, *J* = 7.1 Hz), 4.66 (2H, q, *J* = 7.1 Hz), 8.18 (1H, br s). The spectral data were in good accordance with those reported previously.³⁹

Synthesis of 4-(tert-butyl)-3-hydroxythiazole-2(3H)-thione (4). Zinc chloride (5.2 g, 38.2 mmol) was added to a solution of **15** (3.00 g, 12.7 mmol) in absolute ether (7.5 mL) at such a rate that the solvent did not boil constantly, and then the mixture was stirred at room temperature for 43 hours. Then, 4.0 M HCl (12 mL) was added dropwise to the mixture at 0 °C, and the mixture was stirred for 30 min at room temperature.

The organic materials were extracted with chloroform (3 × 20 mL), and the organic phase was dried over sodium sulfate. After evaporation of the solvent, 0.5 M NaOH (18 mL) was added, and the aqueous solution was washed with chloroform, and then acidified with 4 M HCl (4 mL) to pH = 2. Organic materials were then extracted with chloroform. The resulting organic phase was dried over sodium sulfate. After evaporation of the solvent, the resulting crude product was purified by recrystallization using the dichloromethane/*n*-hexane binary solvent system to afford **4** as beige plates (1.05 g, 72%). ¹H-NMR (chloroform-d, 400 MHz): δ/ppm, 1.42 (9H, s), 6.27 (1H, s), 10.1 (1H, br s). ¹³C NMR (chloroform-d, 100 MHz): δ/ppm, 27.8, 34.4, 100.6, 147.4, 172.0. IR (KBr): ν/cm⁻¹ 3142, 2971, 2938, 2871, 1561, 1434, 1342, 1241, 1096, 994, 760. Anal calcd for C₇H₁₁NOS₂: C, 44.42; H, 5.86; N, 7.40%. Found: C, 44.28; H, 5.62; N, 7.37%.

3-Hydroxy-4,5-dimethylthiazole-2(3H)-thione (5f). Zinc chloride (10.3 g, 75.6 mmol) was added to a solution of **16** (5.07 g, 24.5 mmol) in absolute ether (15.5 mL) at such a rate that the solvent did not boil constantly, and then the mixture was stirred for 49 hours at room temperature. 4.0 M HCl aq. (25 mL) was added dropwise to the mixture at 0 °C, and then the reaction mixture was stirred for 30 min at room temperature. The solution was extracted with CHCl₃ (3 × 20 mL). The organic phase was dried over Na₂SO₄. After evaporation of the solvent, the resulting green residue was purified by column chromatography on silica gel with *n*-hexane/ethyl acetate (2/3, v/v) as eluents to give **5f** as blueish-green solid (2.85 g, 72%). ¹H-NMR (chloroform-d, 400 MHz): δ/ppm, 2.23 (3H, s), 2.29 (3H, s), 9.78 (1H, br s). ¹³C NMR (chloroform-d, 100 MHz): δ/ppm, 11.1, 11.8, 114.9, 130.9, 168.5. IR (KBr): ν/cm⁻¹ 3189, 2881, 2787, 1628, 1539, 1444, 1436, 1371, 1223, 1011. Anal. calcd for C₅H₇NOS₂Zn 0.2H₂O: C, 36.43; H, 4.52; N, 8.50%. Found: C, 36.11; H, 4.46; N, 8.39%.

4-Ethyl-3-hydroxy-5-methylthiazole-2(3H)-thione (5h). A solution of **20**³⁹ (1.12 g, 5.06 mmol) in dichloromethane (18 mL) was added to an ice-cooled solution of potassium hydroxide (1.13 g, 20.1 mmol) in water (20 mL), and the mixture was stirred for 2.5 hours at room temperature. After completion of the reaction, water (5 mL) was added to the reaction mixture, and the organic phase was separated. The aqueous phase was washed with *n*-hexane (2 × 10 mL), and acidified with conc. HCl until pH = 2. Then, the organic materials were extracted with dichloromethane (3 × 10 mL), and the combined organic phase was dried over sodium sulfate. After evaporation of the solvent, the resulting crude product was purified by recrystallization from dichloromethane/*n*-hexane binary solvent system to afford **5h** as blueish-green plates (695 mg, 78%). ¹H-NMR (chloroform-d, 400 MHz): δ/ppm, 1.22 (3H, t, *J* = 7.5 Hz), 2.23 (3H, s), 2.69 (2H, q, *J* = 7.5 Hz), 9.81 (1H, br s). ¹³C NMR (chloroform-d, 100 MHz): δ/ppm, 11.6, 12.5, 19.2, 114.5, 136.0, 168.6. IR (KBr): ν/cm⁻¹ 2973, 2824, 2739, 2656, 1612, 1458, 1371, 1108, 1019, 985, 960, 799. Anal calcd for C₅H₉NOS₂: C, 41.12; H, 5.18; N, 7.99%. Found: C, 41.15; H, 5.03; N, 8.02%.

3-Hydroxy-4,5,6,7-tetrahydrobenzo[d]thiazole-2(3H)-thione (6) (via 14 and 17). Oxime **14** was prepared from 2-chlorocyclohexanone (2.80 g, 21.1 mmol) with hydroxylamine hydrochloride



(1.80 g, 25.9 mmol) and sodium acetate (1.92 g, 23.4 mmol) in a procedure analogous to that for obtaining **12**. The product (**14**) was obtained as a pale-yellow oil (2.83 g) and was directly used in the next step without further purification. Then, **14** (2.83 g, 19.2 mmol) was reacted with potassium *O*-ethylthiocarbonate (3.31 g, 22.7 mmol) in a procedure analogous to that used for the preparation of **16**, with the exception that the reaction time was 2.5 hours, to afford **17** as a yellow oil (4.14 g), which was directly used in the next step without further purification. The obtained **17** was then converted into **6** with zinc chloride (8.01 g, 58.8 mmol) in a procedure analogous to that for obtaining **5f**, with the exception that the reaction time was 66 hours and *n*-hexane/chloroform/ethyl acetate ternary solvent system (2/2/1, v/v/v) was used as eluents for the column chromatography. The product (**6**) was obtained as a blueish-green solid (1.76 g, 45% in 3 steps). ¹H-NMR (chloroform-*d*, 400 MHz): δ /ppm, 1.88 (4H, quint, $J = 2.8$ Hz), 2.53–2.56 (2H, m), 9.73 (1H, br s). ¹³C-NMR (chloroform-*d*, 100 MHz): δ /ppm, 21.1, 22.4, 22.8, 23.3, 100.0, 117.8, 133.4. IR (KBr): ν /cm⁻¹ 2941, 2663, 1621, 1438, 1373, 1357, 1206, 977. Anal. calcd for C₇H₉NOS₂: C, 44.89; H, 4.84; N, 7.48%. Found: C, 44.74; H, 4.78; N, 7.47%.

Synthesis of bis[4-(*tert*-butyl)-3-hydroxythiazole-2(3*H*)-thionolato]zinc(II): Zn(**4**)₂

To a solution of **4** (950 mg, 5.02 mmol) in 50% aqueous ethanol (40 mL) was added Zn(OAc)₂·2H₂O (687 mg, 3.13 mmol) in water (12 mL), and the mixture was stirred for 2 hours at room temperature. The resulting precipitate was collected by filtration and successively washed with water and THF to give white solids, which were purified by recrystallization from dichloromethane/*n*-hexane to give Zn(**5f**)₂ as colorless crystals (908 mg, 82%). ¹H-NMR (chloroform-*d*, 400 MHz): δ /ppm, 1.45 (9H, s), 6.51 (1H, s). ¹³C-NMR (chloroform-*d*, 100 MHz): δ /ppm, 27.6, 34.9, 103.6, 152.1, 160.5. IR (KBr): ν /cm⁻¹ 3135, 3081, 2957, 1558, 1359, 1245, 1032, 685. Anal. calcd for C₁₄H₂₀N₂O₂S₄Zn: C, 38.05; H, 4.56; N, 6.34%. Found: C, 38.01; H, 4.35; N, 6.36%.

Bis[3-hydroxy-4,5-dimethyl-2-thioxo-3-thiazololato]zinc(II): Zn(5f**)₂**. The complex Zn(**5f**)₂ was prepared from **5f** (1.00 g, 6.20 mmol) with Zn(OAc)₂·2H₂O (775 mg, 3.53 mmol) in a procedure analogous to that used for the preparation of Zn(**4**)₂, and was obtained as colorless crystals. (965 mg, 81%). ¹H-NMR (chloroform-*d*, 400 MHz): δ /ppm, 2.28 (3H, s), 2.31 (3H, s). ¹³C-NMR (chloroform-*d*, 100 MHz): δ /ppm, 12.0, 12.4, 117.4, 136.5, 155.6. IR (KBr): ν /cm⁻¹ 3445, 2955, 2918, 1616, 1441, 1396, 1320, 1228, 1093, 1035. Anal. calcd for C₁₀H₁₂N₂O₂S₄Zn: C, 31.13; H, 3.13; N, 7.26%. Found: C, 31.02; H, 3.20; N, 7.14%.

Bis[4-ethyl-3-hydroxy-5-methylthiazole-2(3*H*)-thionolato]zinc(II): Zn(5h**)₂**. The complex Zn(**5h**)₂ was prepared from **5h** (400 mg, 2.28 mmol) with Zn(OAc)₂·2H₂O (277 mg, 1.26 mmol) in a procedure analogous to that used for the preparation of Zn(**4**)₂ and was obtained as colorless needles (373 mg, 79%). ¹H-NMR (chloroform-*d*, 400 MHz): δ /ppm, 1.21 (3H, t, $J = 7.5$ Hz), 2.29 (3H, s), 2.76 (2H, q, $J = 7.5$ Hz). ¹³C-NMR (chloroform-*d*, 100 MHz): δ /ppm, 12.2, 12.5, 19.9, 117.3, 141.6, 155.7. IR (KBr): ν /cm⁻¹ 2969, 2929, 2870, 1610, 1452, 1391, 1312, 1223, 1065, 1038, 1001, 804.

Anal. calcd for C₁₄H₁₆N₂O₂S₄Zn·0.15 H₂O: C, 34.59; H, 3.94; N, 6.73%. Found: C, 34.51; H, 3.91; N, 6.73%.

Bis[3-hydroxy-4,5,6,7-tetrahydrobenzo[*d*]thiazole-2(3*H*)-thionolato]zinc(II): Zn(6**)₂**. The complex Zn(**6**)₂ was prepared from **6** (380 mg, 2.03 mmol) with Zn(OAc)₂·2H₂O (256 mg, 1.17 mmol) in a procedure analogous to that used for the preparation of Zn(**5f**)₂, and was obtained as a pale green solid (332 mg, 75%). ¹H-NMR (chloroform-*d*, 400 MHz): δ /ppm, 1.85 (4H, quint, $J = 2.7$ Hz), 2.57–2.61 (4H, m), 2.71–2.74 (4H, m). ¹³C-NMR (chloroform-*d*, 100 MHz): δ /ppm, 21.3, 23.0, 23.4, 23.8, 120.8, 138.5, 156.4. IR (KBr): ν /cm⁻¹ 2946, 1614, 1439, 1387, 1300, 1206, 1033, 1011. Anal. calcd for C₁₄H₁₆N₂O₂S₄Zn·0.15 H₂O: C, 38.16; H, 3.73; N, 6.36%. Found: C, 38.07; H, 3.62; N, 6.25%.

X-ray crystallographic analysis

X-ray data for Zn(**3**)₂ with pyridine were collected on a Rigaku XtaLAB P200 diffractometer with multi-layer mirror monochromated MoK α ($\lambda = 0.71073$ Å) and a hybrid photon counting detector (PILATUS 200K). The crystal structure was solved by direct methods (SHELXT Version 2014/5)⁴⁰ and refined by full-matrix least-squares SHELXL-2014/7.⁴¹ All non-hydrogen atoms were refined anisotropically. All hydrogen atoms were located from difference electron density maps.

X-ray data for Zn(**4**)₂, Zn(**5f**)₂, Zn(**5h**)₂, Zn(**6**)₂, and Zn(**5h**)₂ with pyridine were collected on a Bruker SMART APEX II ULTRA diffractometer equipped with graphite monochromated MoK α radiation ($\lambda = 0.71073$ Å) generated by a rotating anode. The cell parameters for the compounds were obtained from a least-squares refinement of the spot. Data collection, data reduction and semi-empirical absorption correction were carried out using the software package of APEX2.⁴² All of the calculations for the structure determination were carried out using the SHELXTL package.⁴¹ In all cases, nonhydrogen atoms were refined anisotropically and hydrogen atoms were placed in idealized positions and refined isotropically in a riding manner along with their respective parent atoms.

In vitro insulin-mimetic activity

Male Wistar rats were sacrificed under anesthesia with ether. The adipose tissues were removed, chopped with scissors and digested with collagenase for 60 min at 37 °C in Krebs Ringer bicarbonate buffer (120 mM NaCl, 1.27 mM CaCl₂, 1.2 mM MgSO₄, 4.75 mM KCl, 1.2 mM KH₂PO₄, 24 mM NaHCO₃; pH 7.4) containing 2% bovine serum albumin. The adipocytes were then separated from undigested tissues and washed with the buffer three times. The isolated adipocyte solutions were preincubated at 37 °C for 30 min with various concentrations of the zinc(II) complexes or ZnSO₄ in saline containing 5 mM glucose. Then, an epinephrine solution was added to the reaction mixtures (final concentration; 10 mM), and the resulting solutions were incubated at 37 °C for 3 h. The reactions were stopped by soaking in ice water, and the mixtures were centrifuged at 3000 rpm at 4 °C for 10 min. FFA levels in the outer solution of the cells were determined with an FFA kit (NEFA C-test Wako, Wako Pure Chemicals, Osaka, Japan). All animal



experiments in the present study were approved by the Experimental Animal Research of Kyoto Pharmaceutical University (KPU) and were performed according to the Guideline for Animal Experimentation of KPU.

Determination of log *P* values by reversed-phase HPLC analysis

An HPLC analysis was performed on a Mightysil RP-18 GP II column (particle size: 5 μm, 4.6 mm i.d. × 250 mm, KANTO CHEMICAL Co., Inc., Japan) with an SSC-3461 pump (SENSHU SCIENTIFIC Co., Ltd, Japan), SSC-2300 column oven (SENSHU SCIENTIFIC Co., Ltd, Japan), and 875-UV Intelligent UV/VIS detector (JASCO Co., Ltd, Japan). Eluents: 80%(v/v) methanol in water, Flow rate: 0.7 mL/min, Detection: 254 nm, and Column oven temperature: 35 °C. Tartrazine was used as an unretained compound to determine the dead time (*t*₀). A series of standard compounds including phenol (log *P* = 1.46), benzene (log *P* = 2.13), bromobenzene (log *P* = 2.99), naphthalene (log *P* = 3.37), biphenyl (log *P* = 3.98), phenanthrene (log *P* = 4.57) were analyzed to generate a calibration curve (Fig. S2, ESI†).⁴³

Determination of acid dissociation constants (p*K*_a) of the ligands

The pH values of aqueous solutions containing the ligands were measured using a composite electrode GST-5841C (DKK-TOA Corp., Japan) and a multi-water quality meter MM-60R (DKK-TOA Corp., Japan). Compounds were dissolved in a THF-water mixture in 20 ml (Adjusted to be approximately 0.004 M) and neutralization titrated with 0.01 M sodium hydroxide solution (*f* = 1.001, KANTO CHEMICAL CO., INC.) prepared in any THF concentration. The p*K*_a was determined from the half-equivalence point. Titrations were performed with different THF-water ratios (THF: 40.0, 50.0, 66.7%), and the p*K*_a in water was determined by three-point extrapolation.

Determination of the stability constants (log *K*) of the zinc(II) complexes

The pH was measured using a composite electrode GST-5841C (DKK-TOA Corp., Japan) and a multi-water quality meter MM-60R (DKK-TOA Corp., Japan). A THF solution of the ligand is mixed with an aqueous solution of zinc ions and the pH is measured. The overall stability constant was determined by calculation from the hydrogen ion concentration. All THF concentrations were 50%. The acid dissociation constant “*K*_a” at that concentration was determined experimentally.

Author contributions

R. Saito: writing – original draft, conceptualization, data curation, funding acquisition, investigation, methodology, project administration, resources, supervision, visualization. Y. Naito: data curation, formal analysis, investigation, resources, validation, visualization, writing – review and editing. Y. Yoshikawa: data curation, formal analysis, investigation, resources, validation, visualization, writing – review and editing. H. Yasui: methodology, project administration, resources, supervision,

validation, writing – review and editing. S. Kikkawa: data curation, formal analysis, investigation, resources, validation, visualization, writing – review and editing. R. Ohba: data curation, formal analysis, investigation, visualization. T. Miyamoto: data curation, formal analysis, investigation, visualization. S. Sano: data curation, formal analysis, investigation, visualization. K. Maeda: data curation, formal analysis, investigation, visualization. M. Tamura: data curation, formal analysis, investigation, visualization. I. Azumaya: investigation, resources, validation, writing – review and editing.

Data availability

Relevant crystal data collection and refinement data for the crystal structures are summarized in Table S1 (ESI†). CCDC 2379130 (for Zn(3)₂), 2383333 (for Zn(4)₂), 2383335 (for Zn(5f)₂), 2383331 (for Zn(5f)₂ + pyridine), 2383324 (for Zn(5h)₂), and 2383338 (for Zn(6)₂) contain the supplementary crystallographic data for this paper.

Conflicts of interest

The authors declare that they have no competing interests that could have appeared to influence this study.

Acknowledgements

This research was supported by JSPS KAKENHI Grant Number JP25410179. The authors would like to thank Editage (<https://www.editage.jp>) for English language editing.

References

- H. Sun, P. Saeedi, S. Karuranga, M. Pinkepank, K. Ogurtsova, B. B. Duncan, C. Stein, A. Basit, J. C. N. Chan, J. C. Mbanya, M. E. Pavkov, A. Ramachandaran, S. H. Wild, S. James, W. H. H. Herman, P. Zhang, C. Bommer, S. H. Kuo, E. J. J. Boyko and D. J. Magliano, *Diabetes Res. Clin. Pract.*, 2022, **183**, 109119.
- World Health Organ. *Tech. Rep. Ser.*, 1985, vol. 727, pp. 1–113.
- A. F. Amos, D. J. McCarty and P. Zimmet, *Diabet. Med.*, 1997, **14**, S7–S85.
- B. Lorenzati, C. Zucco, S. Miglietta, F. Lamberti and G. Bruno, *Pharmaceuticals*, 2010, **3**, 3005–3020.
- E. Standl and M. Füchtenbusch, *Diabetologia*, 2003, **46**, M30–M36.
- W. Kaim and B. Schwederski, *Bioinorganic Chemistry: Inorganic Elements in the Chemistry of Life: An Introduction and Guide*, John Wiley & Sons Ltd, Chichester, UK, 1994.
- G. J. Fosmire, *Am. J. Clin. Nutr.*, 1990, **51**, 225–227.
- J. Wolf, H. H. Sandstead and L. Rink, in *Handbook on the Toxicology of Metals*, ed. G. F. Nordberg and M. Costa, Academic Press, 5th edn, 2022, ch. 38, pp. 963–984, DOI: [10.1016/B978-0-12-822946-0.00034-9](https://doi.org/10.1016/B978-0-12-822946-0.00034-9).



- 9 L. I. Stiles, K. Ferrao and K. J. Mehta, *Clin. Exp. Med.*, 2024, **24**, 38–56.
- 10 L. Coulston and P. Dandona, *Diabetes*, 1980, **29**, 665–667.
- 11 M. Nishida, H. Sakurai, J. Kawada, M. Koyama and J. Takada, *Naturwissenschaften*, 1989, **76**, 220–222.
- 12 J. Fugono, H. Yasui and H. Sakurai, *J. Pharm. Pharmacol.*, 2002, **54**, 611–615.
- 13 Y. Yoshikawa, E. Ueda, Y. Kojima and H. Sakurai, *Life Sci.*, 2004, **75**, 741–751.
- 14 Y. Yoshikawa, A. Murayama, Y. Adachi, H. Sakurai and H. Yasui, *Metallomics*, 2011, **3**, 686–692.
- 15 Y. Naito, Y. Yoshikawa and H. Yasui, *Bull. Chem. Soc. Jpn.*, 2011, **84**, 298–305.
- 16 M. Yamaguchi, R. Saito, Y. Adachi, Y. Yoshikawa, H. Sakurai and A. Katoh, *Heterocycles*, 2007, **73**, 603–615.
- 17 A. Groggs, N. Schneiders, K. Daniel, T. Gottwald and J. Hartung, *Tetrahedron*, 2008, **64**, 10882–10889.
- 18 J. M. Hatcher, M. C. Kohler and D. M. Coltart, *Org. Lett.*, 2011, **13**, 3810–3813.
- 19 D. H. R. Barton, D. Crich and G. Kretschmar, *J. Chem. Soc., Perkin Trans. 1*, 1986, 39–53, DOI: [10.1039/p19860000039](https://doi.org/10.1039/p19860000039).
- 20 S. Lou and G. C. Fu, *J. Am. Chem. Soc.*, 2010, **132**, 1264–1266.
- 21 K. K. K. Goh, S. Kim and S. Z. Zard, *Org. Lett.*, 2013, **15**, 4818–4821.
- 22 Z. R. He, Z. Y. Zhang, K. Asare-Yeboah and S. Bi, *Mater. Adv.*, 2023, **4**, 769–786.
- 23 A. D. Bond, F. Benevelli and W. Jones, *J. Mater. Chem.*, 2002, **12**, 324–332.
- 24 M. Nakai, H. Watanabe, C. Fujiwara, H. Kakegawa, T. Satoh, J. Takada, R. Matsushita and H. Sakurai, *Biol. Pharm. Bull.*, 1995, **18**, 719–725.
- 25 M. Yamaguchi, K. Wakasugi, R. Saito, Y. Adachi, Y. Yoshikawa, H. Sakurai and A. Katoh, *J. Inorg. Biochem.*, 2006, **100**, 260–269.
- 26 H. Kawarada, Y. Yoshikawa, H. Yasui, S. Kuwahara, Y. Habata and R. Saito, *Metallomics*, 2011, **3**, 675–679.
- 27 R. Saito, M. Tamura, S. Kawano, Y. Yoshikawa, A. Kato, K. Sasaki and H. Yasui, *New J. Chem.*, 2017, **41**, 5572–5581.
- 28 Y. Yoshikawa, E. Ueda, Y. Suzuki, N. Yanagihara, H. Sakurai and Y. Kojima, *Chem. Pharm. Bull.*, 2001, **49**, 652–654.
- 29 M. Calvin and K. W. Wilson, *J. Am. Chem. Soc.*, 1945, **67**, 2003–2007.
- 30 H. Freiser, R. G. Charles and W. D. Johnston, *J. Am. Chem. Soc.*, 1952, **74**, 1383–1385.
- 31 J. Bjerrum, *Metal Ammine Formation in Aqueous Solution: Theory of the Reversible Step Reactions*, ed. P. Haase, 1957.
- 32 K. Suzuki, M. Yasuda and K. Yamasaki, *Bull. Chem. Soc. Jpn.*, 1957, **75**, 229–231.
- 33 H. M. Irving and H. S. Rossotti, *J. Chem. Soc.*, 1941, 2904–2910.
- 34 K. K. Mui, W. A. E. McBryde and E. Nieboer, *Can. J. Chem.*, 1974, **52**, 1821–1833.
- 35 S. Castellano, D. Kuck, M. Viviano, J. Yoo, F. López-Vallejo, P. Conti, L. Tamborini, A. Pinto, J. L. Medina-Franco and G. Sbardella, *J. Med. Chem.*, 2011, **54**, 7663–7677.
- 36 I. T. Papadas, S. Fountoulaki, I. N. Lykakis and G. S. Armatas, *Chem. – Eur. J.*, 2016, **22**, 4600–4607.
- 37 T. Yasukawa, K. Sakamoto, Y. Yamashita and S. Kobayashi, *ACS Catal.*, 2022, **12**, 5887–5893.
- 38 R. Buchman, R. A. Komoroski, K. M. Kauppila, J. J. Mannion and L. Gehrlein, *J. Agric. Food Chem.*, 1985, **33**, 896–907.
- 39 EP249328, 1987.
- 40 G. M. Sheldrick, *Acta Crystallogr., Sect. A: Found. Adv.*, 2015, **71**, 3–8.
- 41 G. M. Sheldrick, *Acta Crystallogr., Sect. C: Struct. Chem.*, 2015, **71**, 3–8.
- 42 *APEX2 Version 2009.1-0 Data collection and Processing Software*, Bruker AXS Inc., Madison, WI, 2008.
- 43 R. Saito, A. Ohno and E. Ito, *Tetrahedron*, 2010, **66**, 583–590.

